Micro-gravity measurements for different purposes in volcanology and tectonics

by
Gerhard Jentzsch

November 19, 2014

The 60th anniversary (1954-2014) of the start of gravity measurements in Strasbourg by R. Lecolazet

Outline:

1. Introduction to micro-gravity measurements
2. Example 1: Volcanology
3. Example 2: Groundwater variation
4. Example 3: Tectonic research in Antarctica (feasibility study)
5. A new gravimeter for precise measurements: The Burris meter

Micro-gravimetry at volcanoes –some basics

The most spectacular example: Campi Flegrei, Italy – the so-called Serapis Temple and the elevation and gravity changes

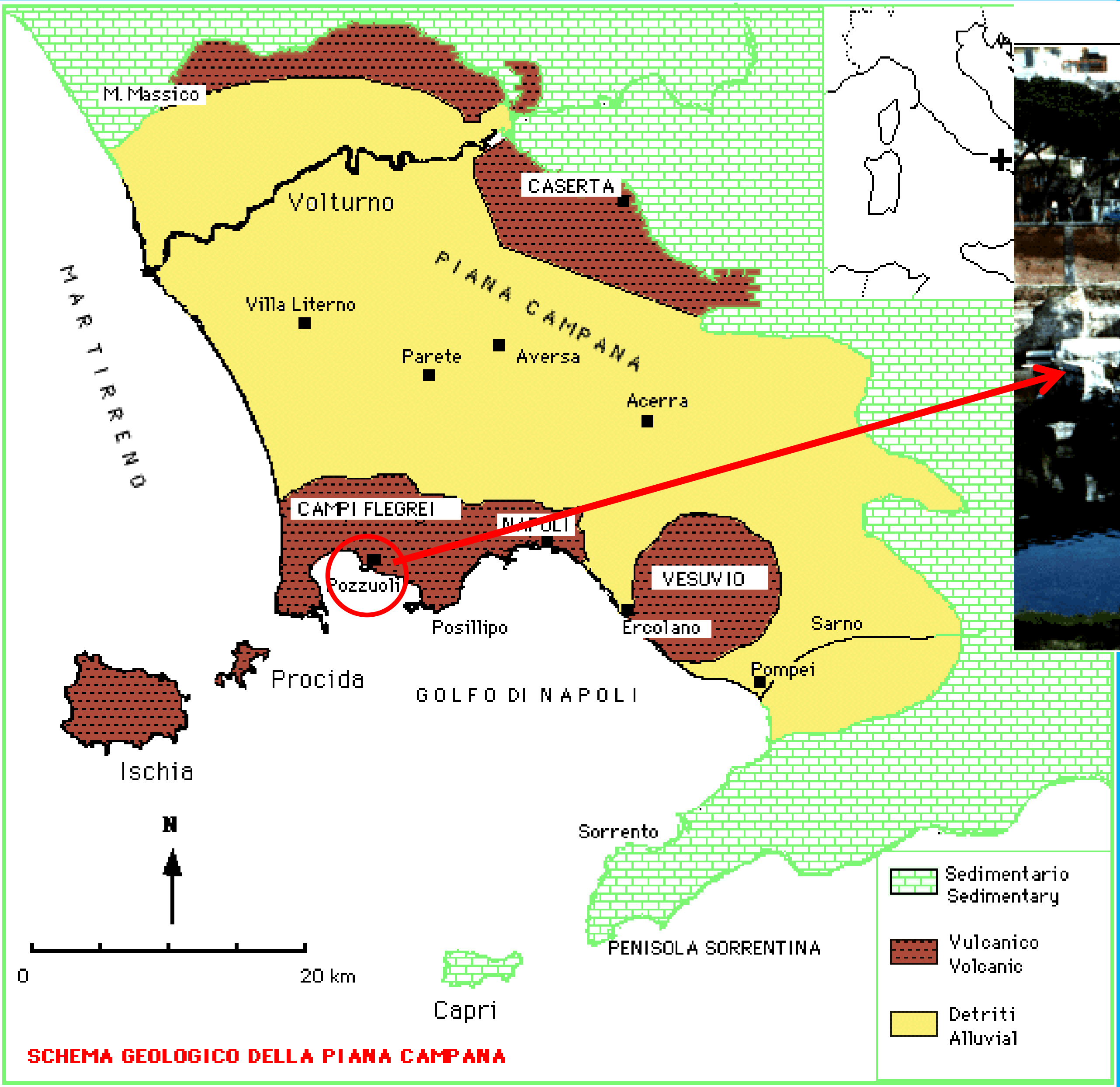

The old market place Puzzuoli

(Campi Flegrei homepage)

Tilling and Dvorak (1993)

Photo taken in the year 1970

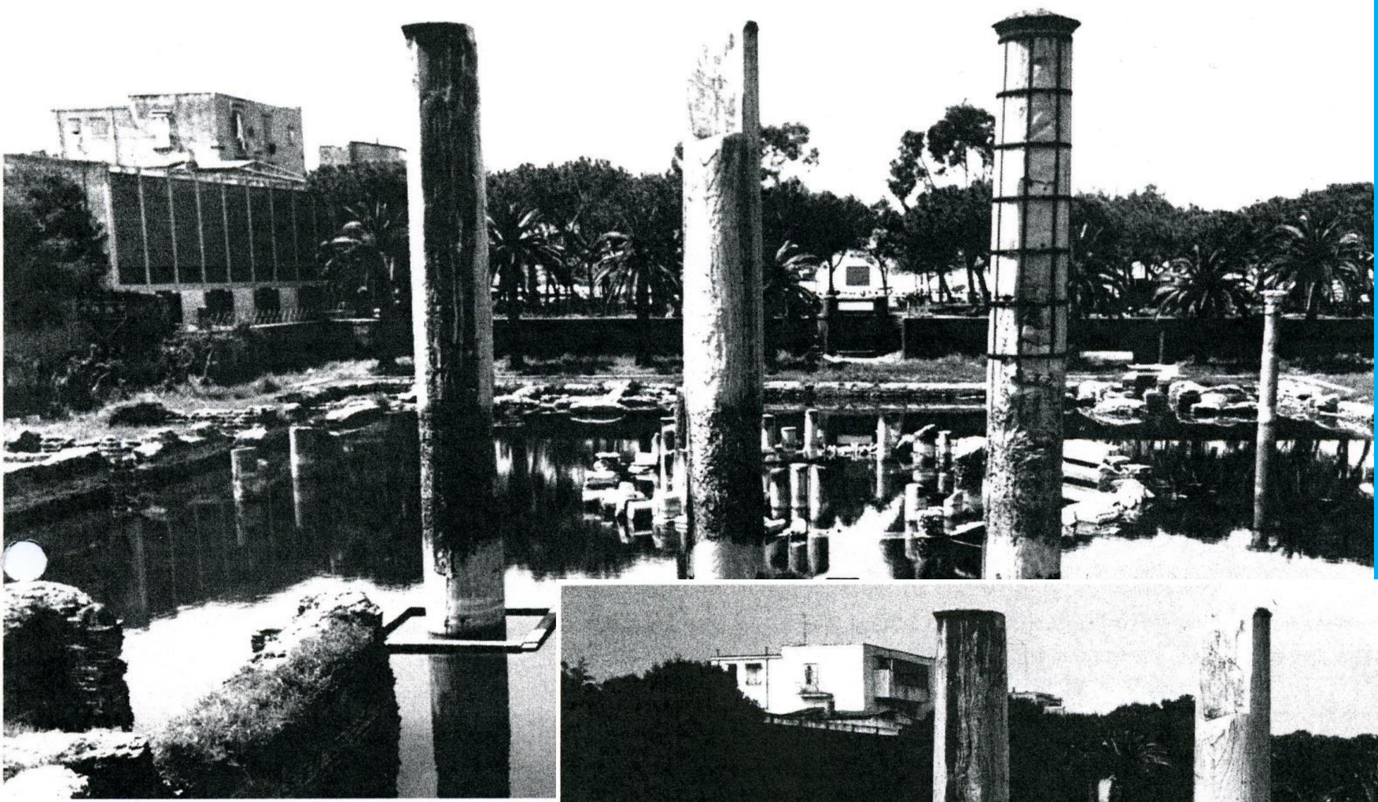

Figure 19. Photograph of Serapis ta
submergence of this monument. At th
of the three wells built around each o

and in 1986:

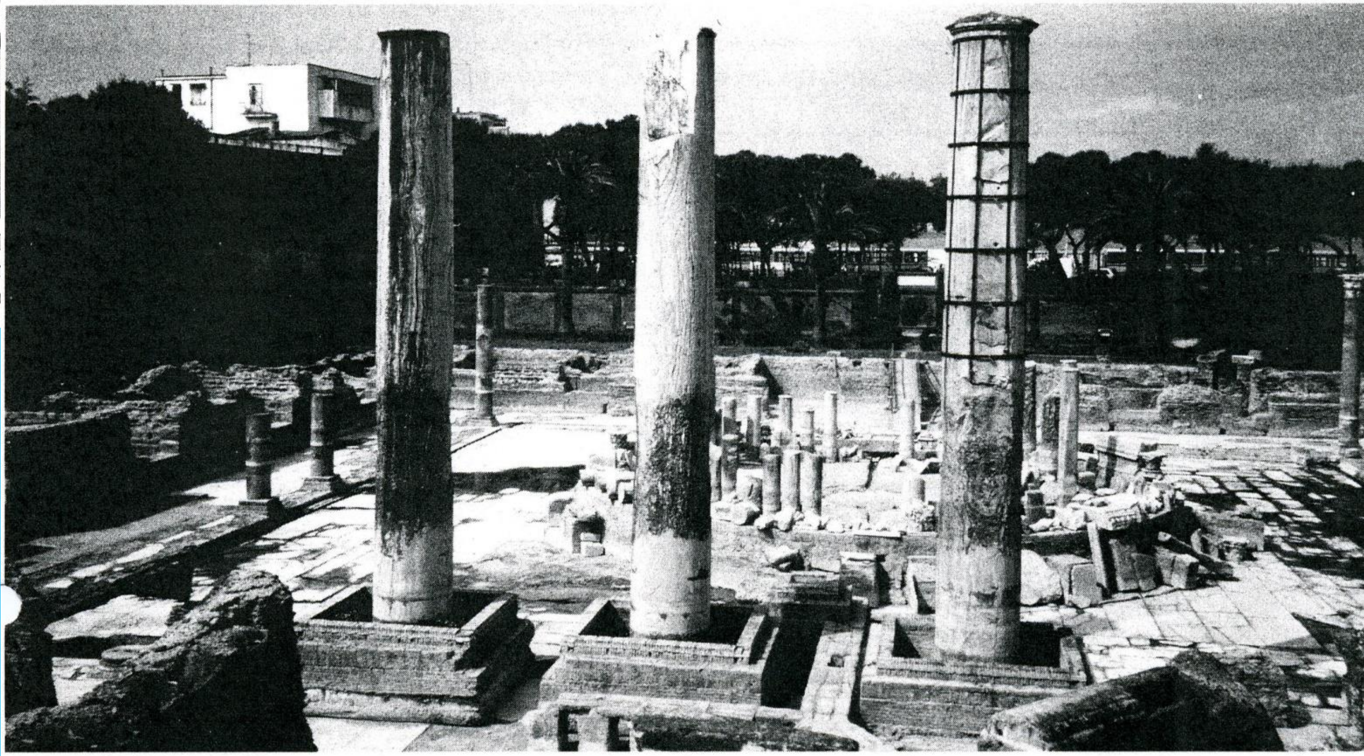

Figure 20. Photograph of Serapis taken in June 1986. Two uplift episodes since 1968 have raised the floor so that it is once again "dry and free of debris."

Derivation of subsidance and uplift related to the sea surface

erosion due to breakwater
and sea shells / worms

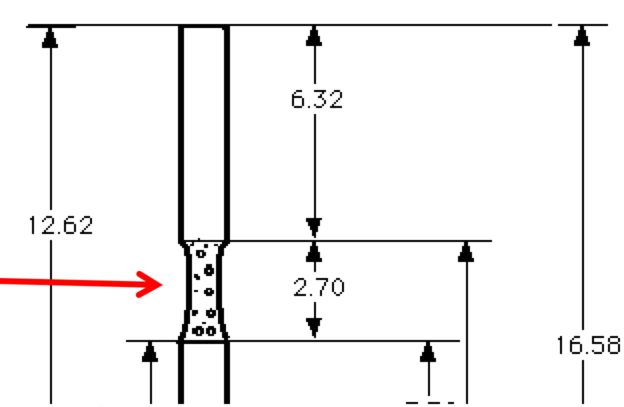

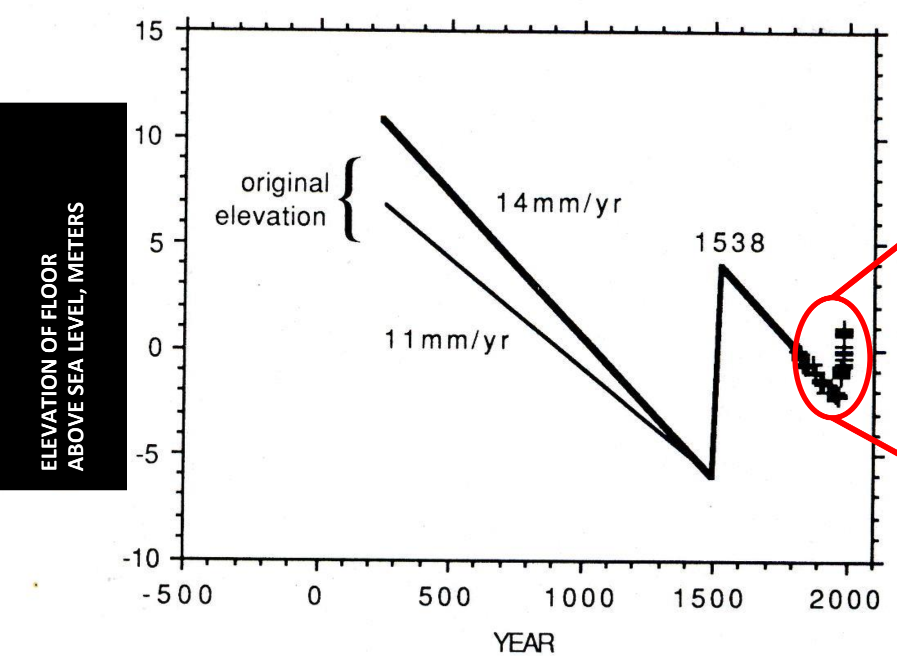

Figure 26. History of vertical movement at Serapis. Measurements from the 1820s to 1986 are the same as shown in Figure 21. Extrapolation of a subsidence rate of 14 mm/yr suggests that the floor of Serapis may have been about 4 m above sea level after the 1538 eruption in Campi Flegrei. If Serapis reached its maximum subsidence of 7 m below sea level during the 15th century, then uplift of about 11 m occurred during the few decades before the 1538 eruption. Based on eyewitness accounts, uplift of a few meters occurred the two days immediately before the eruption. A constant subsidence rate of 11 mm/yr, which is within the uncertainty determined from data shown in Figure 21, can account for our estimate of 5 to 10 m for the original elevation of the tiled marble floor of Serapis.

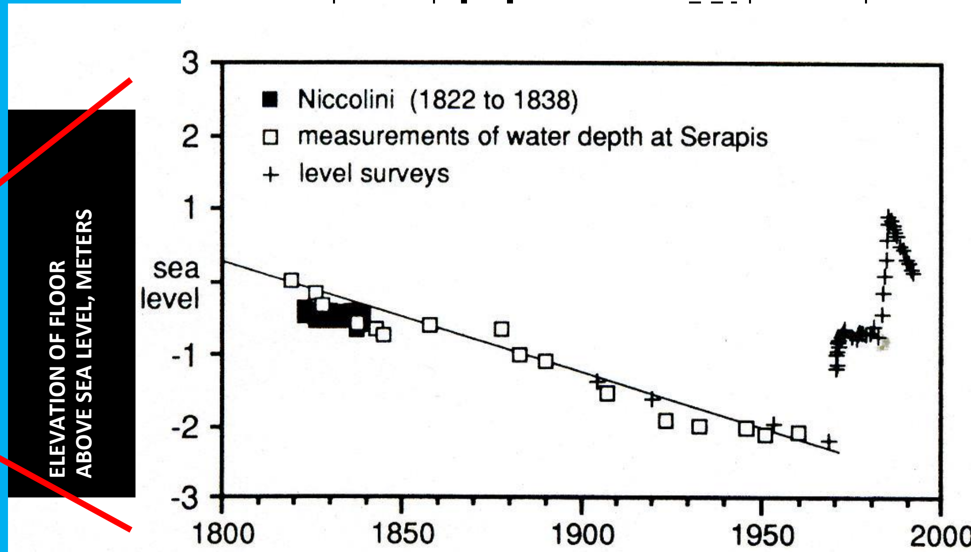

Figure 21. Measurements of the elevation of the floor of Serapis relative to sea level. Open squares denote water depth on the floor measured by different visitors to Serapis between 1819 and 1960 (listed in Table 3). Solid squares indicate that the elevation was determined by leveling surveys, reported by Digiesi (1954) and Corrado and Palumbo (1969). The cluster of solid symbols between 1822 and 1838 are weekly measurements of water depth at Serapis made by Niccolini (1839), shown in more detail in Figure 13. Triangles are elevations determined by leveling surveys conducted from March 1970 to October 1986 (Zugiani, 1972; Berrino and others, 1984). The solid line is a linear least-squares line (slope = 14 [± 3] mm/yr) fitted to only data that are plotted as open squares.

Correlation of gravity and elevation changes:

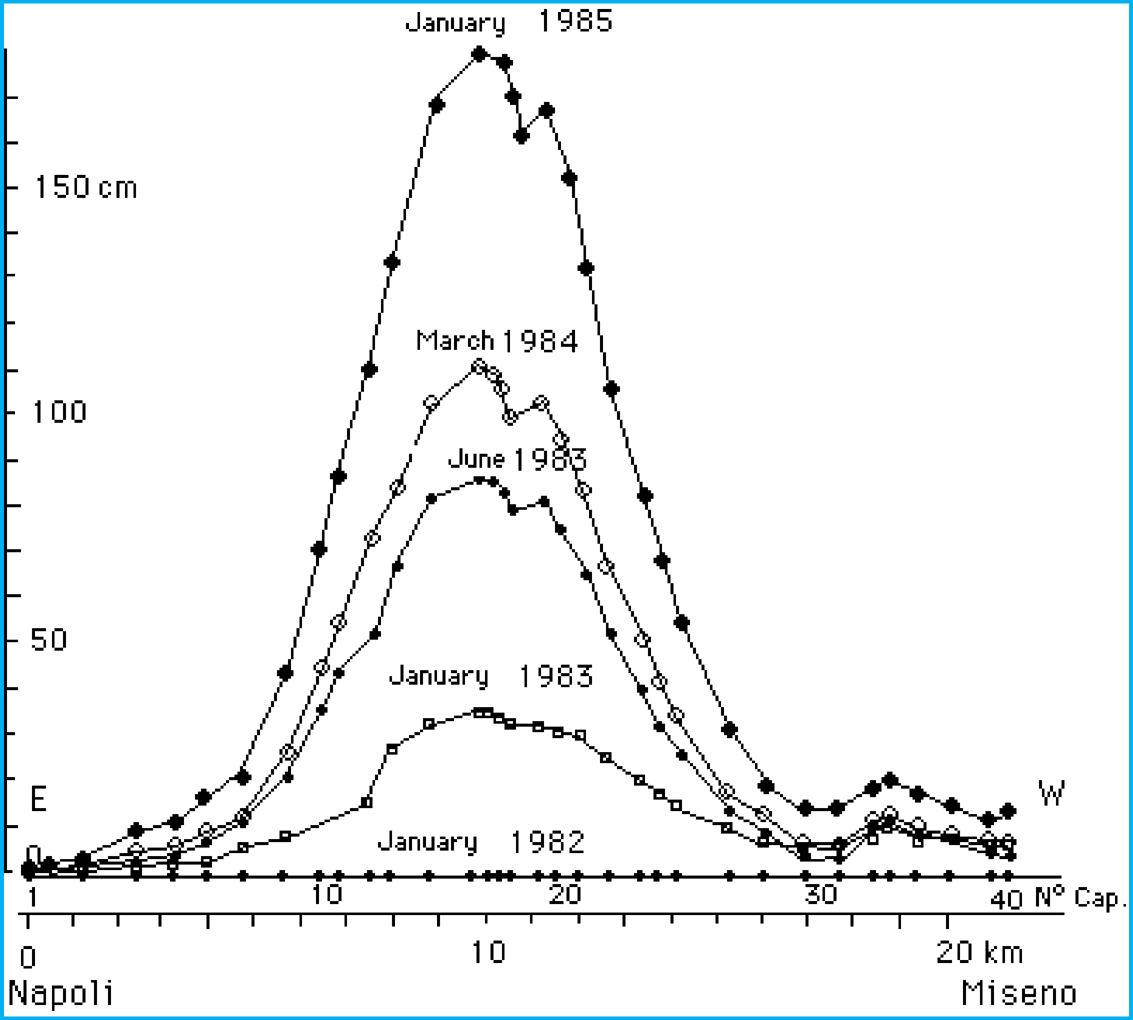

Deformation crises of the years 1982 to 1985 along the Gulf of Pozzuoli.

(Campi Flegrei homepage)

The vertical gradient for Puzzuoli:

Note the strong correlation of elevation and gravity changes, the free-air gradient and the residual gravity changes;

But, the deviation from the expected changes containes the information about the ongoing processes.

(Trasatti and Bonafede)

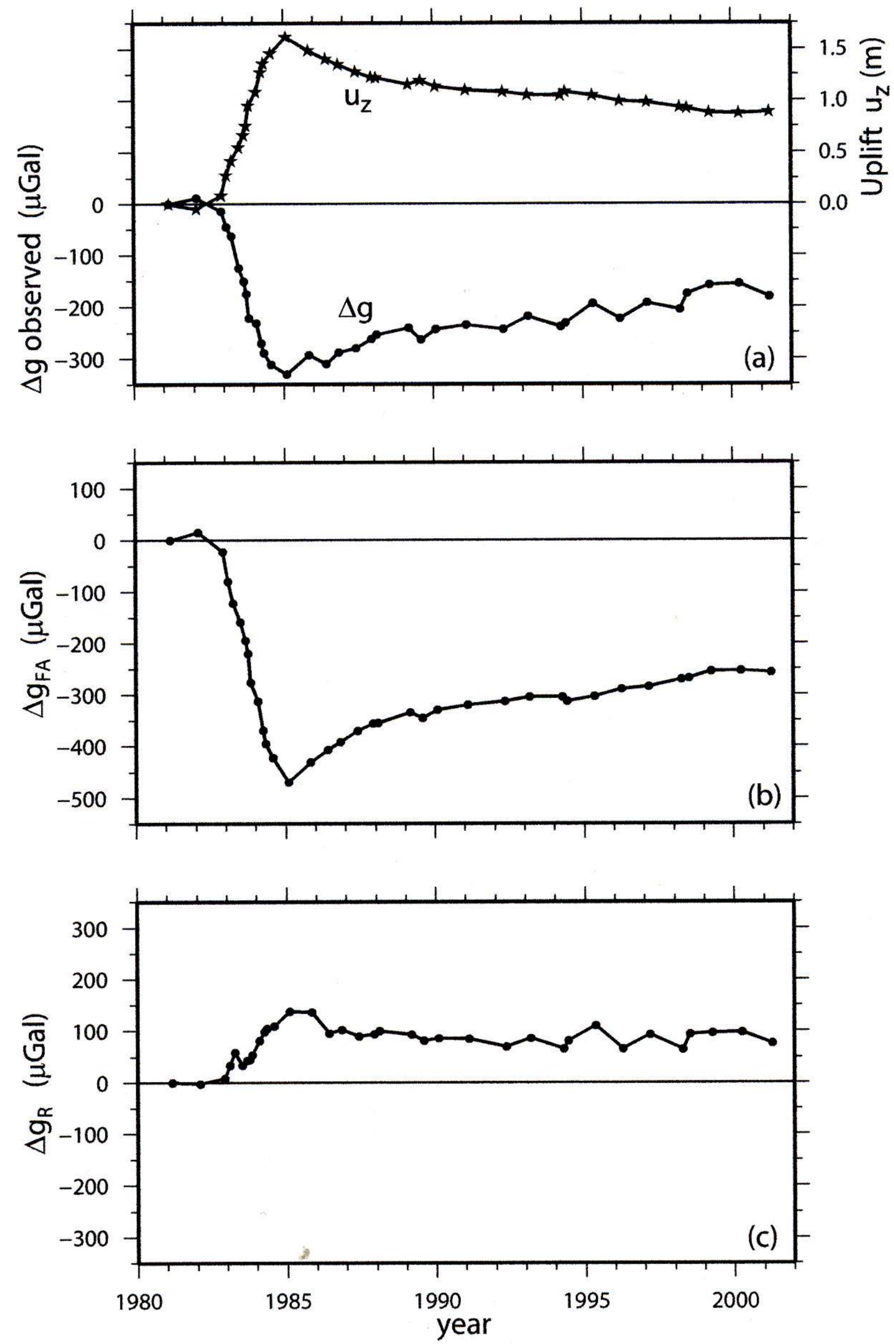

Micro-gravimetry and deformation – basic relations:

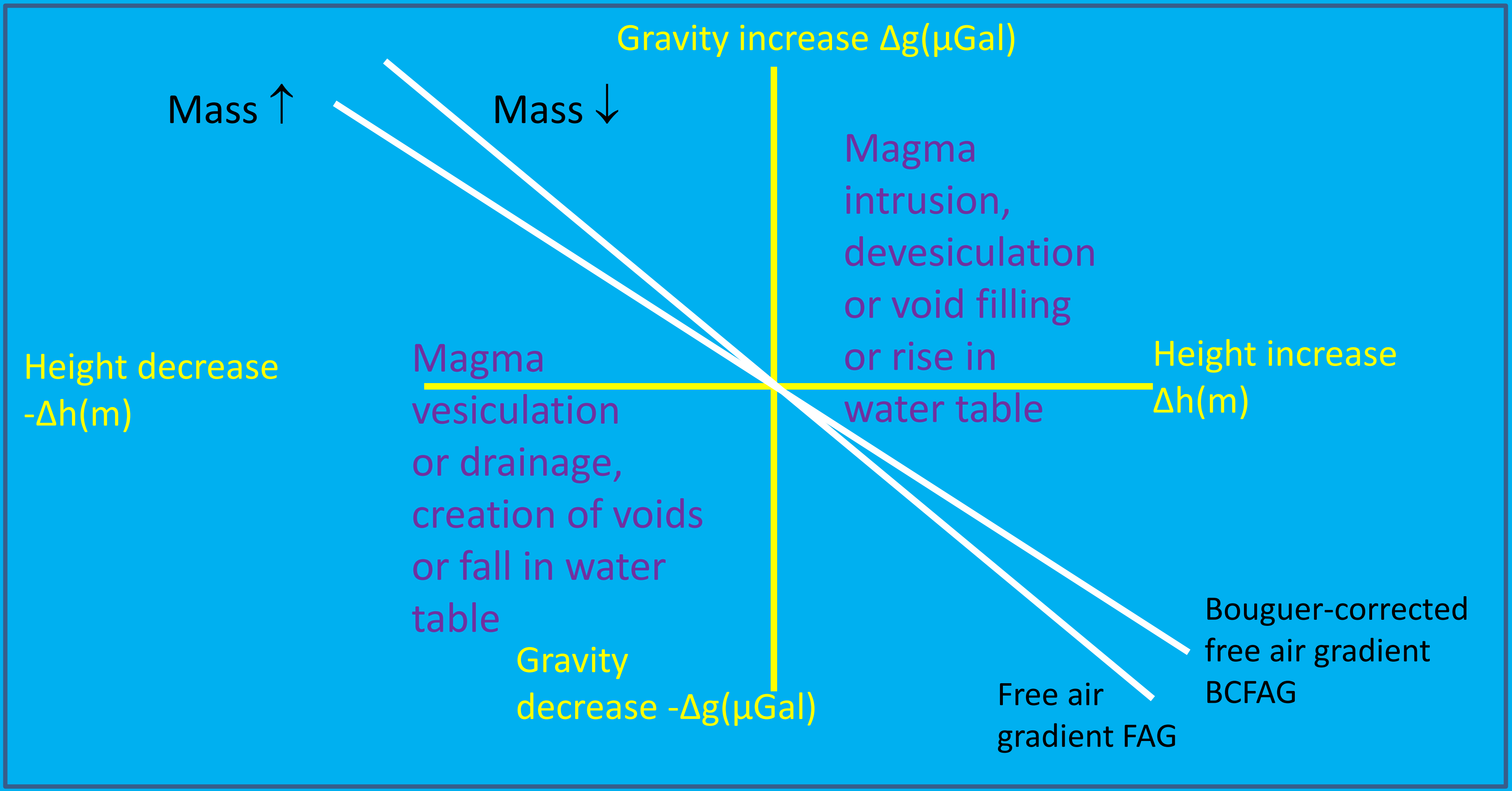

nach Rymer (1996), vergl. Scarpa and Tilling (1996)

Another example shows contrary behaviour:

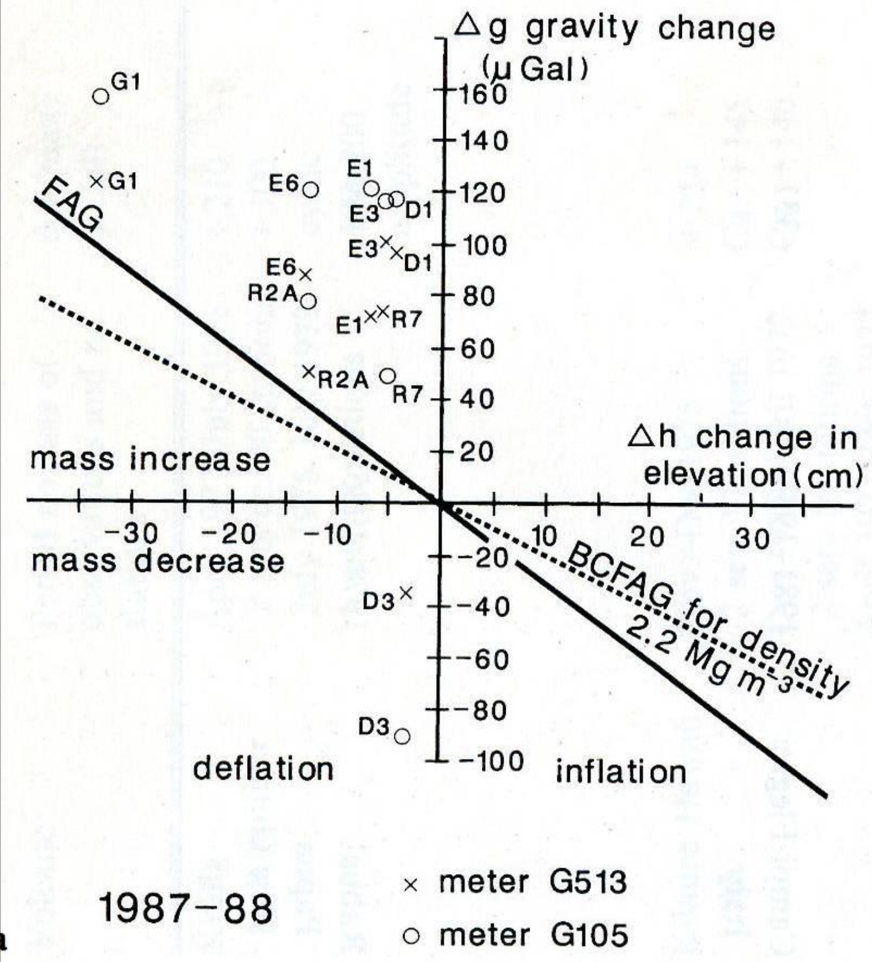

Especially andesitic volcanoes
Provide gravity variations
without the expected elevation
changes !

Fig. 5. Gravity–height variations observed at Poas volcano, Costa Rica between March 1987 and March 1988. Inset shows station locations. (After Rymer and Brown 1989)

Mayon volcano, Philippines:

eruption 1984

3. Micro-gravity network and measurements

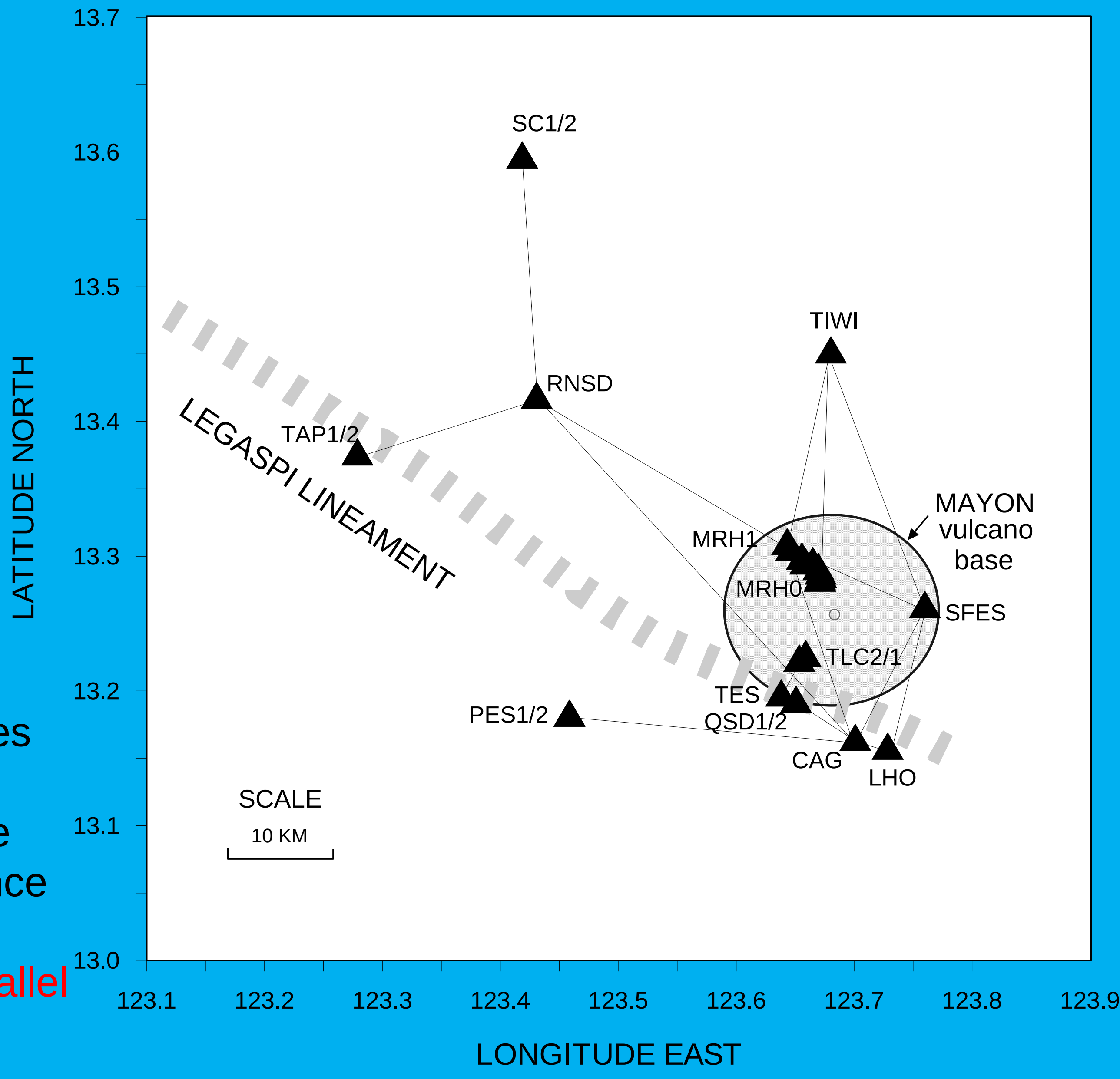

In all:
16 stations along the profiles MRH and TLC
3 points as local reference
7 points as distant reference

3 gravimeters used in parallel

Pictures of our points around Mayon:
Some points are easy to reach, others not …

Cagsawa church, destroyed 1814

On the way uphill to Mayon Resthouse and the observatory

… carrying the gravimeters along an active lahar channel …

Note red arrows marking the way: The lower one from the current year, the upper one from the year before …

GPS measurements on a lahar protection dam – gravity point on the foot of the dam.

Measurements on a school yard in a small village: Always lots of spectators …

4. Observed variations:

Significant gravity changes but no significant elevation changes (note error bars)

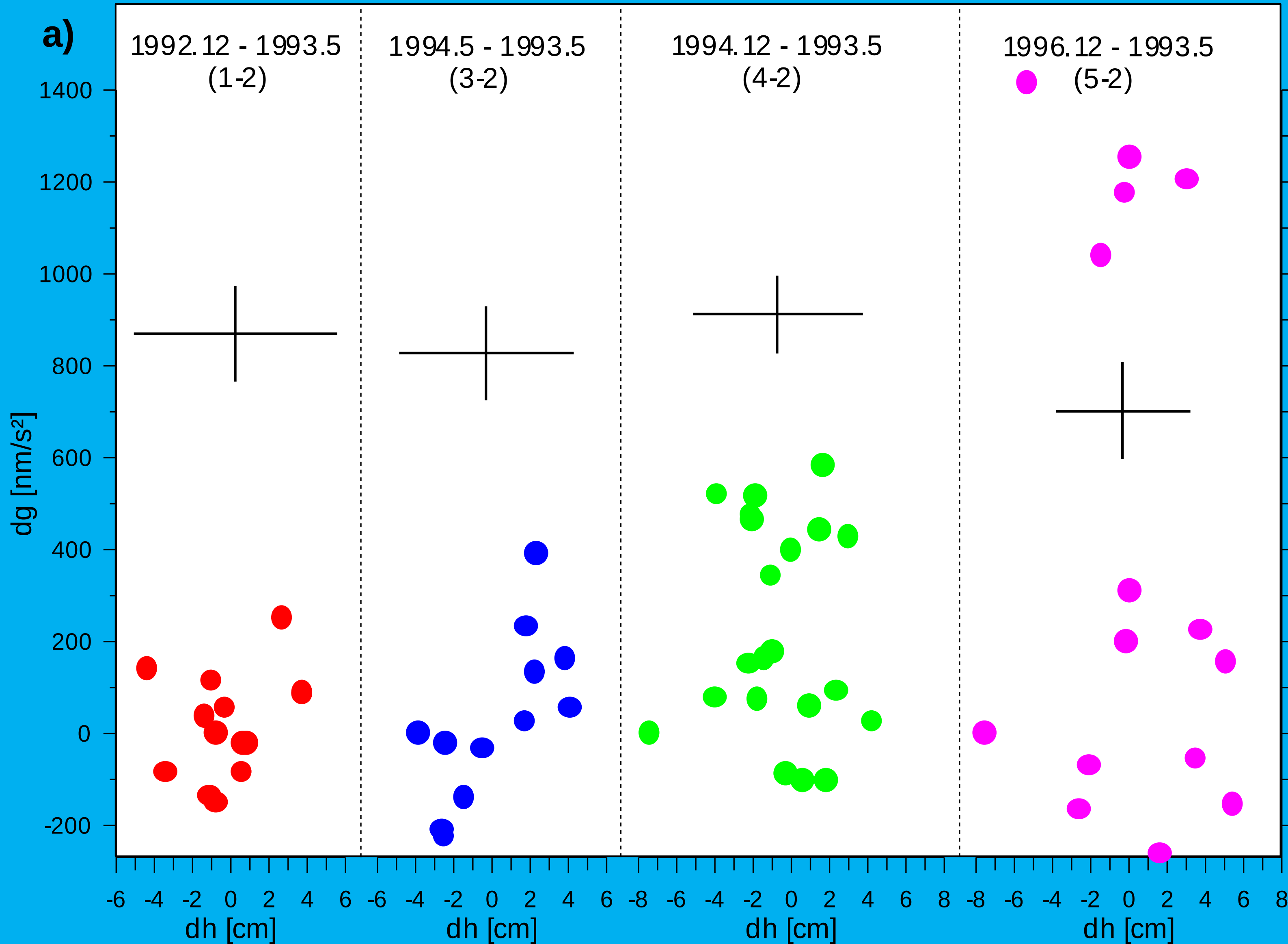

Obtained gravity variations for both profiles:

Mayon Resthouse (MRH)

and

Tumpa Lahar Channel (TLC)

Note:
Variations are restricted to the area of the volcano (radius < 8 km).

MRH had more points due to the road uphill, but many were lost after reconstruction.

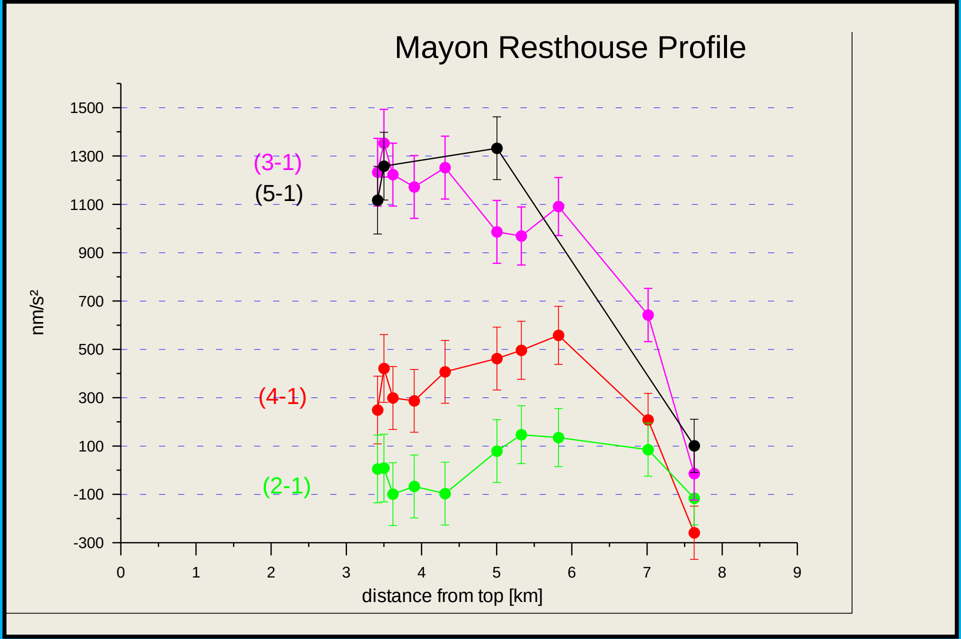

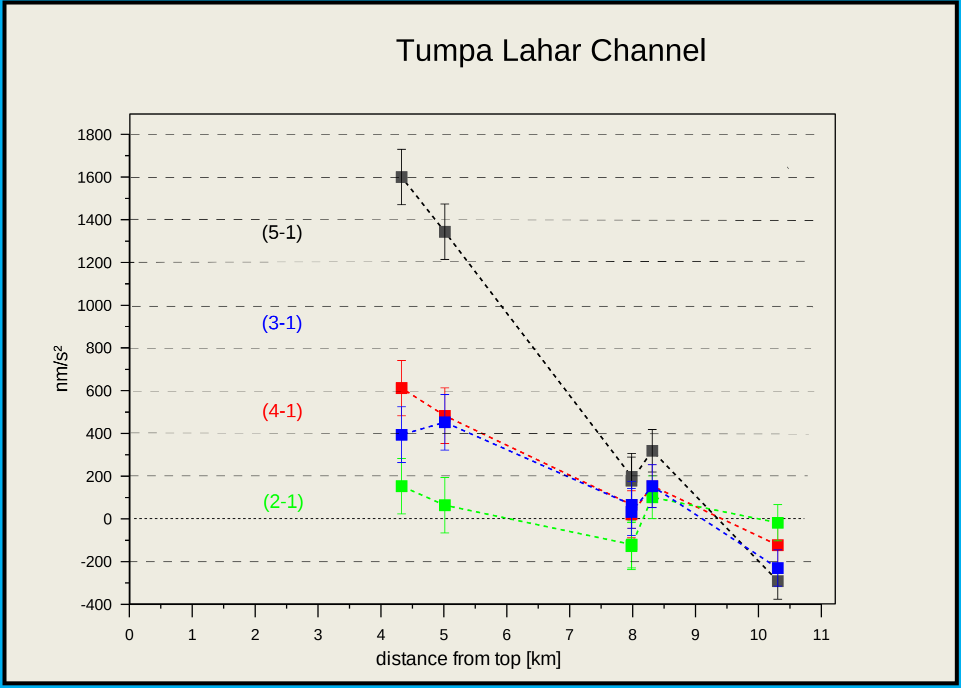

5. Our simple model:

DEFLATION

Basic idea: After the first campaign Mayon erupted in February 1993. Thus, we expected to monitor decreasing activities, although the gravity variations increased.

The only explanation possible was redistribution of mass from above our network to below; thus, we assumed a process in the volcanic vent.

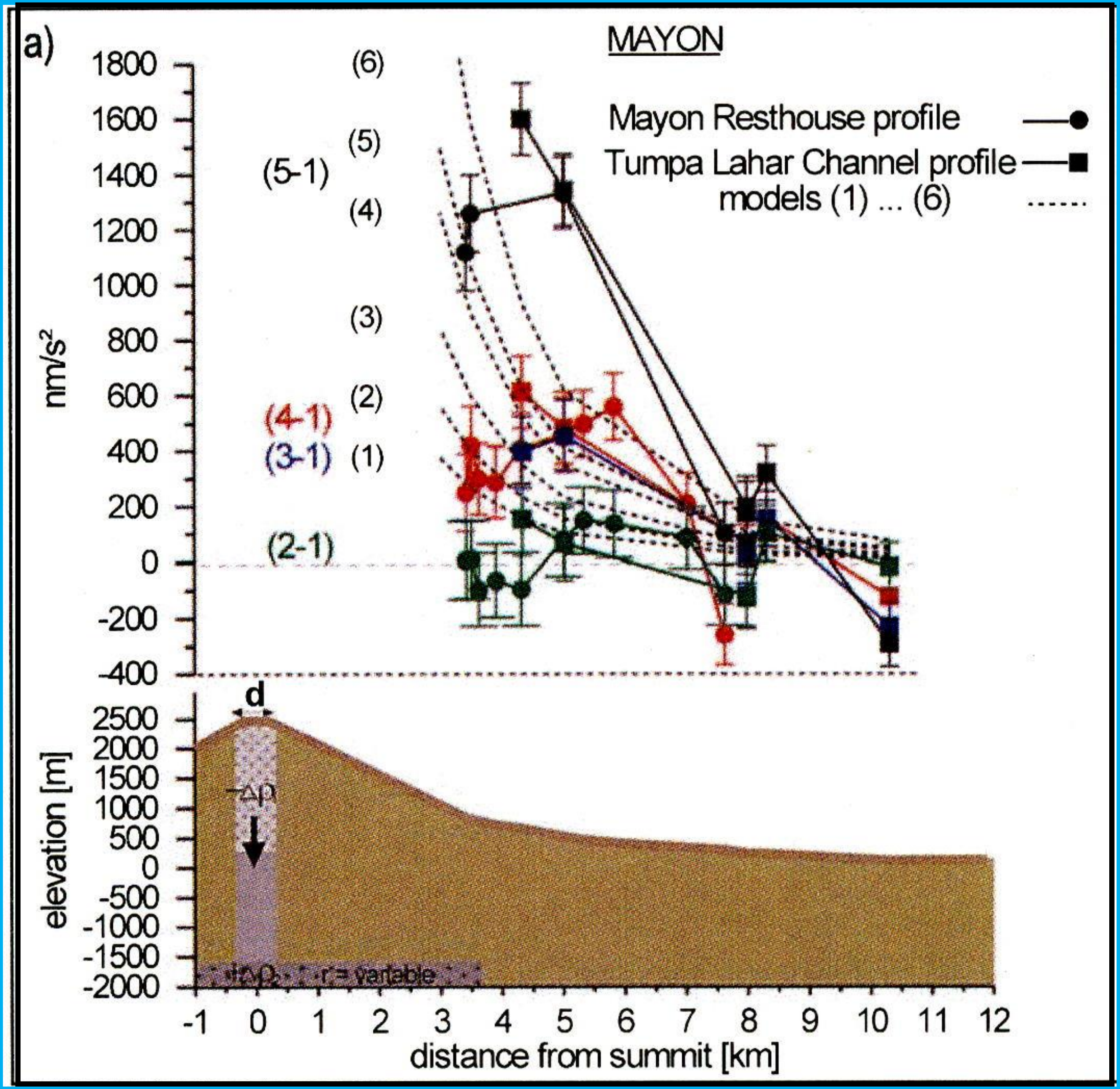

The model and its parameters

Table: Model parameters for the vent – radius and density differences.

model version	1	2	3	4	5	6	max. observed [nm/s²]
Radius [m]	**200**	**200**	**300**	**300**	**400**	**400**	
Density difference [kg/m³]	**400**	**600**	**400**	**600**	**400**	**600**	
Tumpa Lahar Channel [nm/s²]	**155**	**233**	**349**	**524**	**621**	**931**	**1579**
Mayon Resthouse [nm/s²]	**297**	**445**	**668**	**1002**	**1188**	**1782**	**1339**

Comparison of observations for both profiles with the different models; note the consistency of both data sets and the difference to the modelling results.

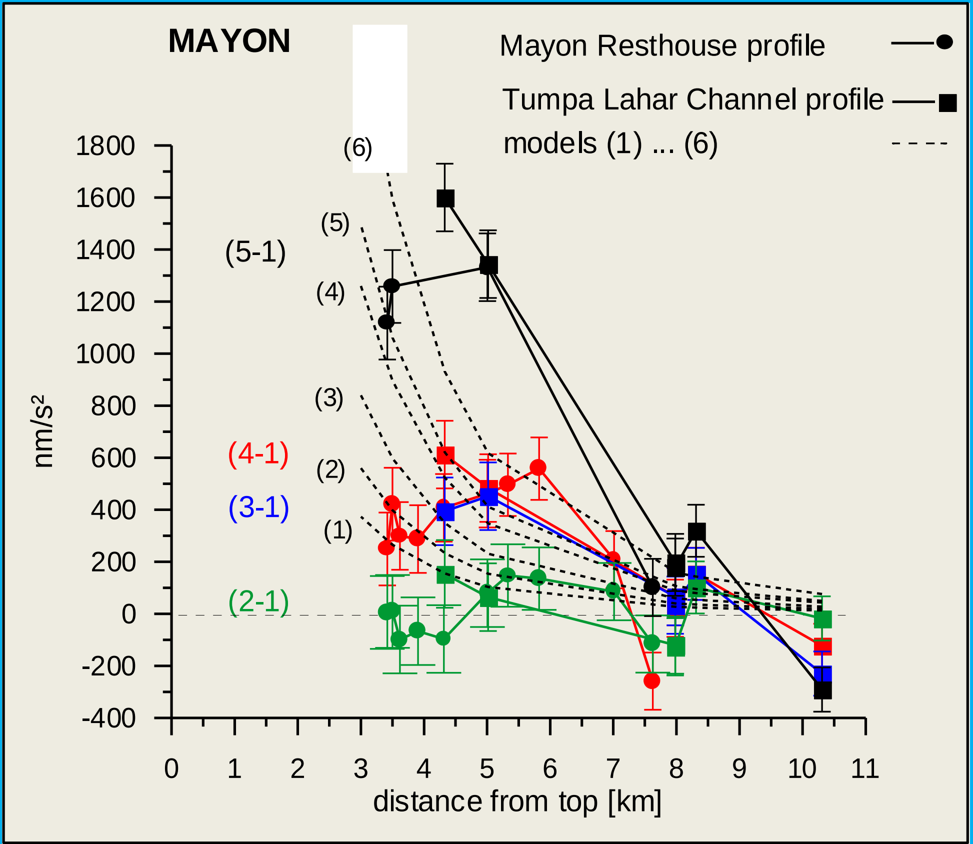

Geodynamic Observatory Moxa:

Investigation of the local water storage system with regard to global data to correct the SG-data for local effects;

Therefore, a local network of points was Installed, and **up to six** well calibrated gravimeters with feed-back were used in parallel during each campaign.

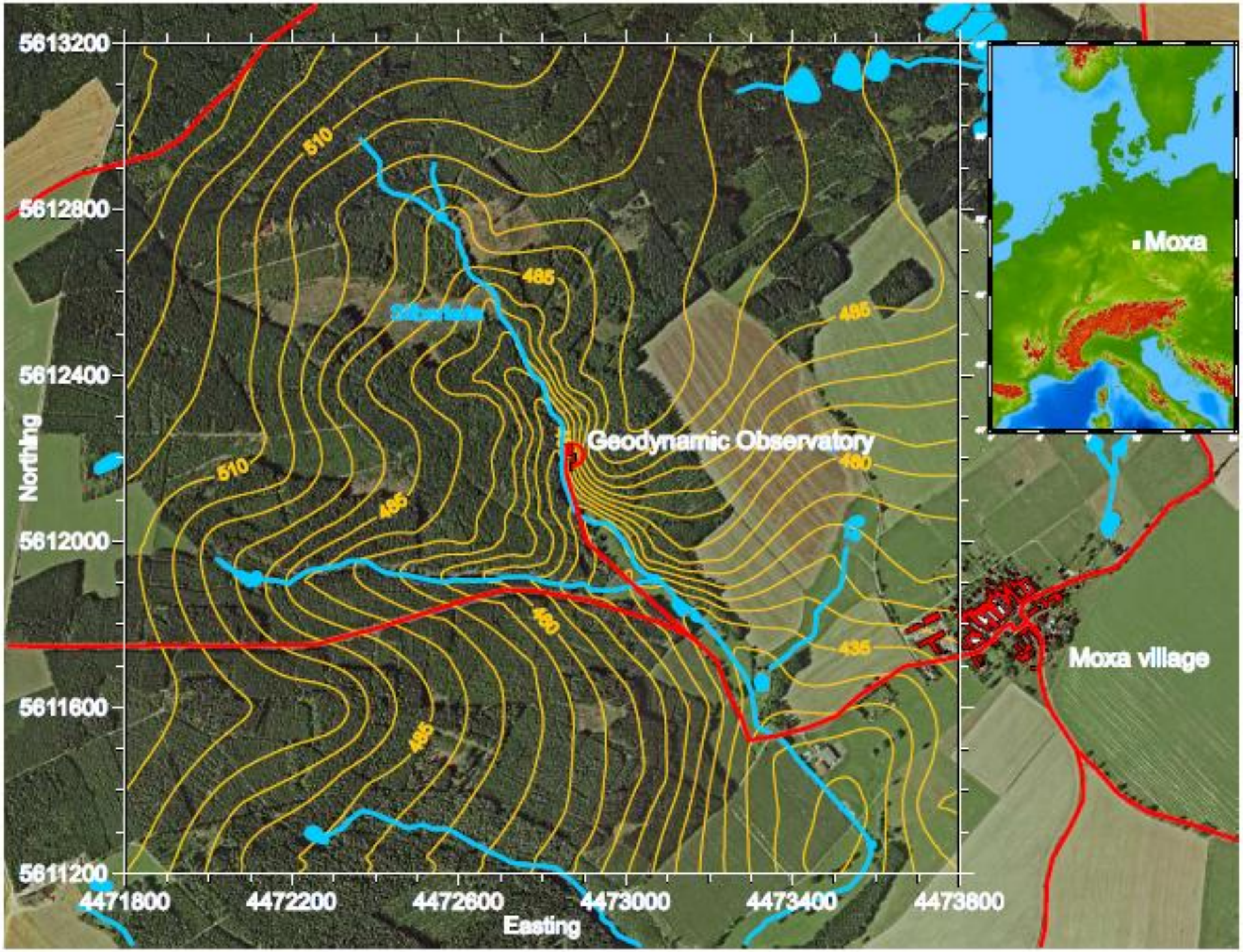

Figure 2.1: Location of the Geodynamic Observatory Moxa in Europe as well as topographic and geographic features in its surroundings. The aerial photograph was taken from Google Earth (2008).

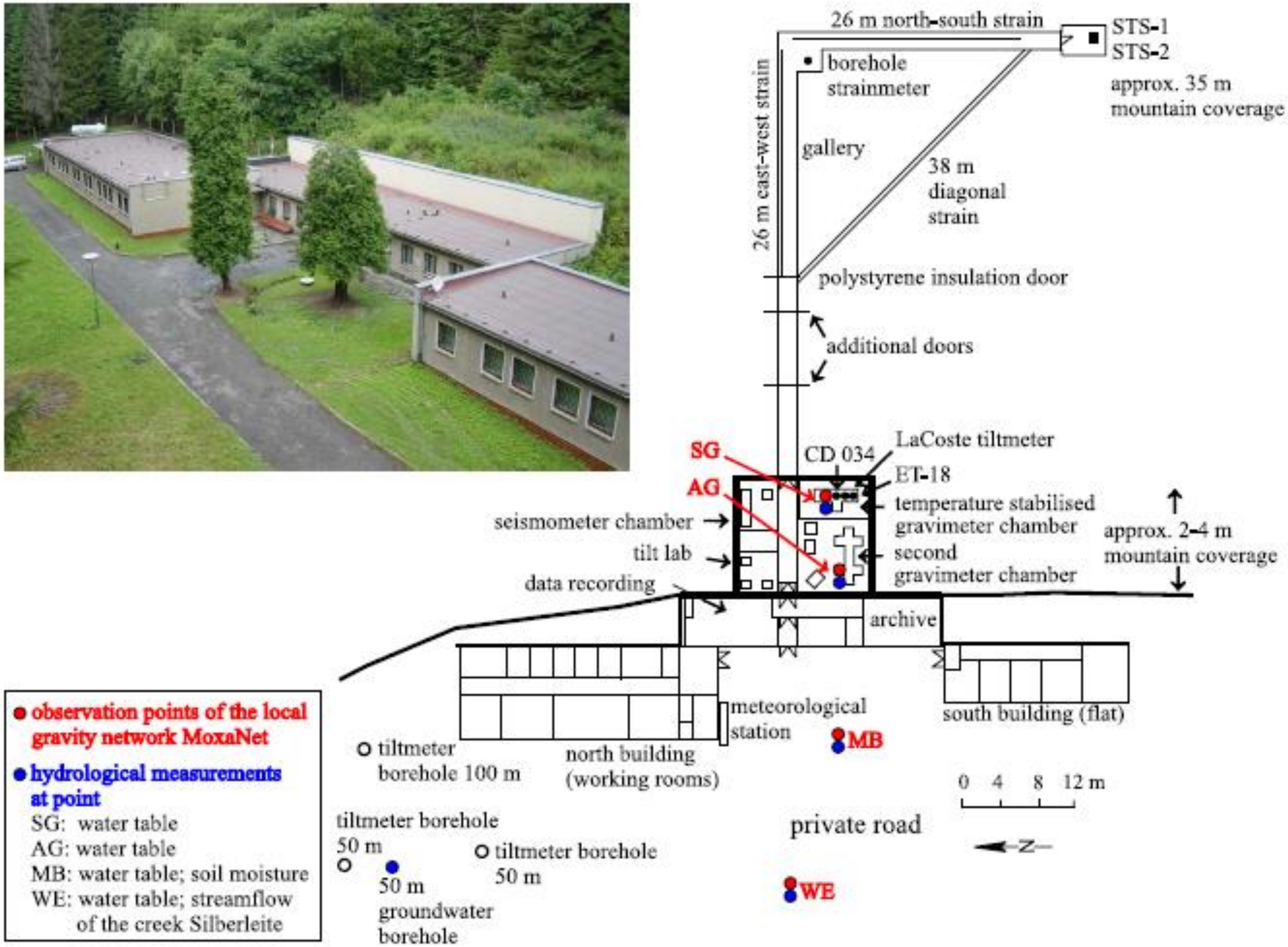

Figure 2.2: Floor plan of the Geodynamic Observatory Moxa showing all important facilities (Schulze, 1998, modified). Additionally, some points of the local gravity network MoxaNet (Section 3.3.1) are given in red and the positions of local hydrological sensors are marked in blue.

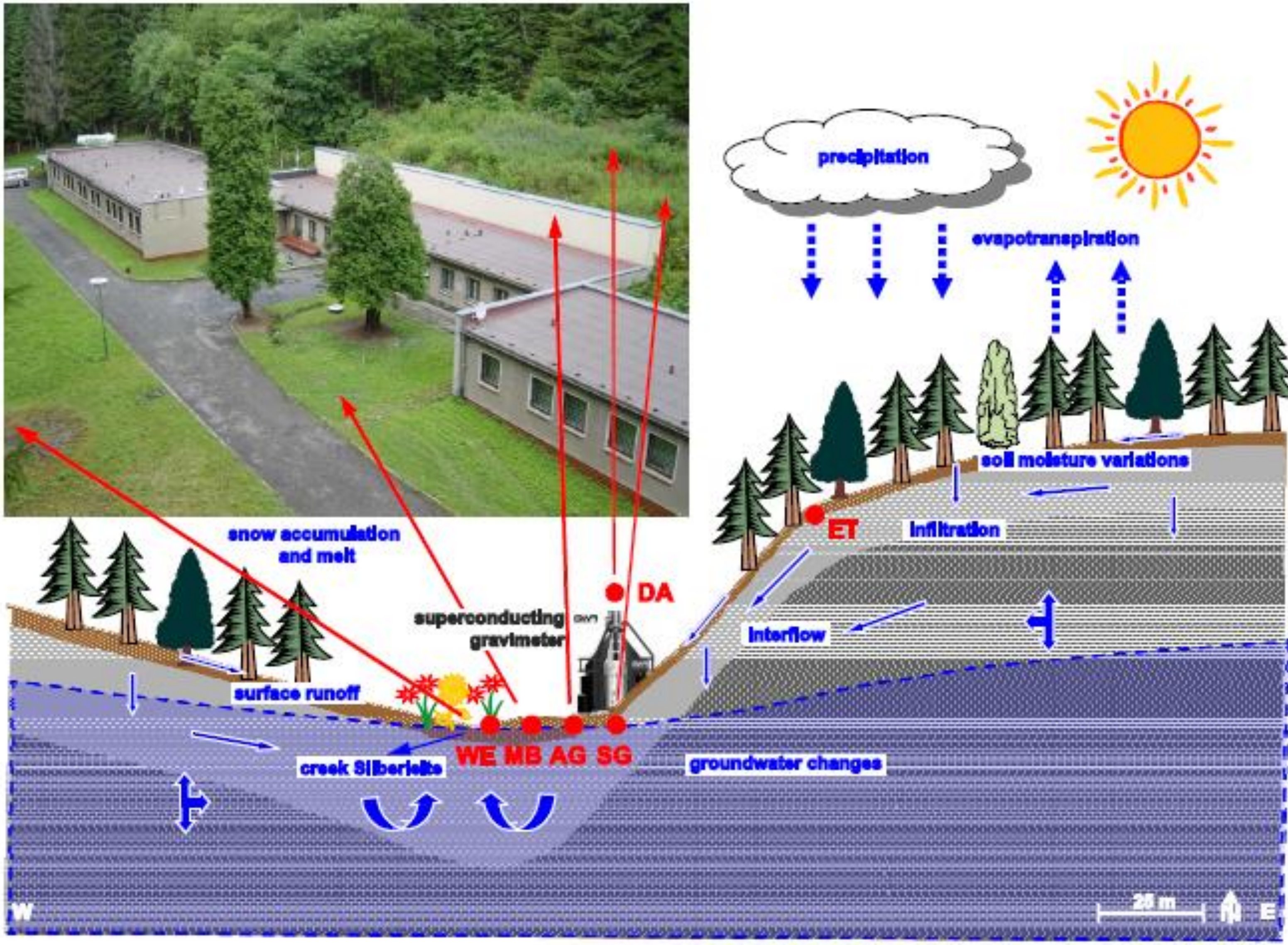

Figure 2.8: Sketch of the hydrological processes and flow paths at Moxa observatory, and location of the superconducting gravimeter and the observation points in the local gravity network MoxaNet (red points, Section 3.3).

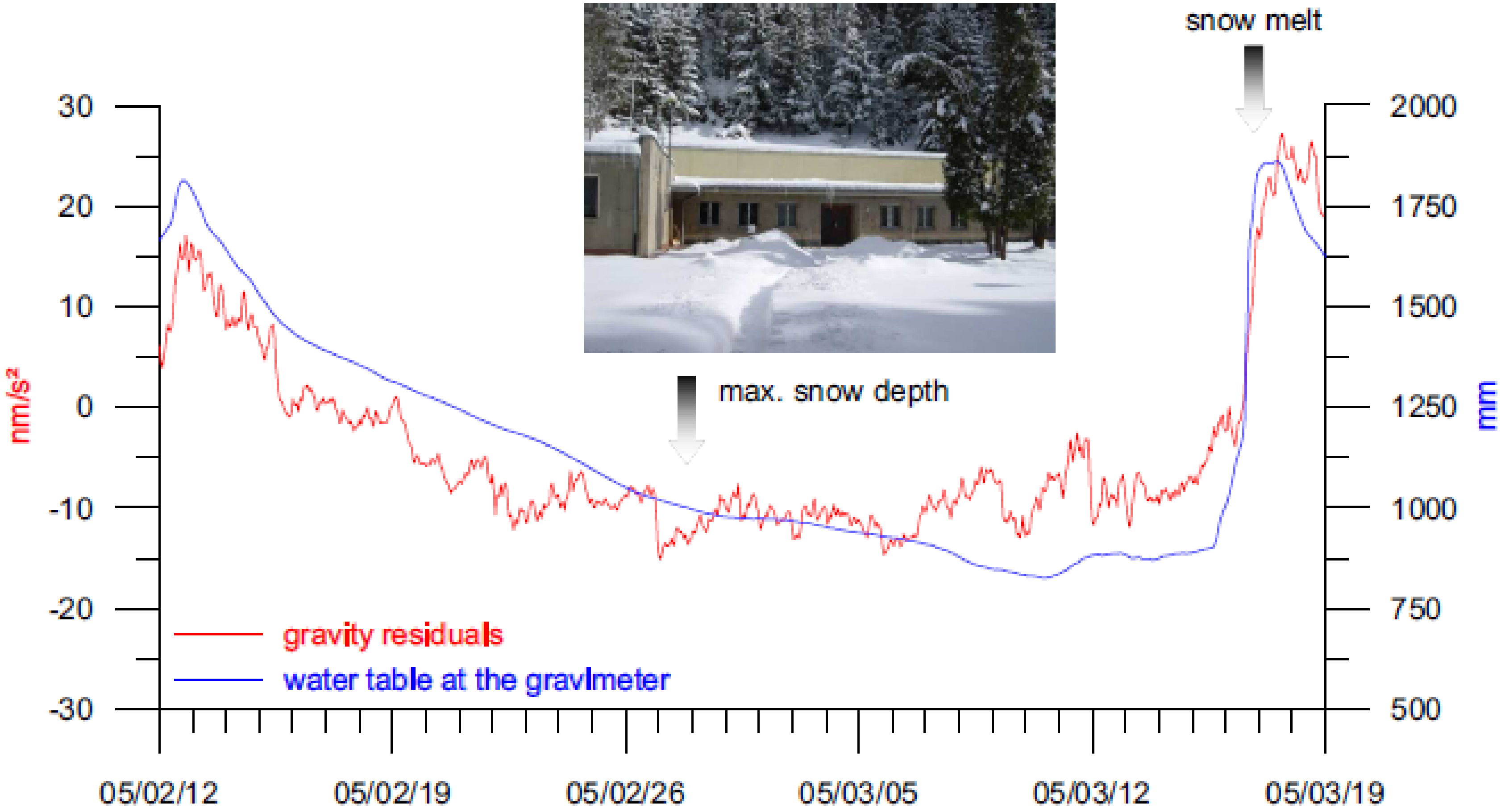

Figure 3.2: Influence of snow accumulation and melt on the observations with the superconducting gravimeter at Moxa. Shown are the gravity residuals and the water table at the gravimeter site (Kroner, 2006).

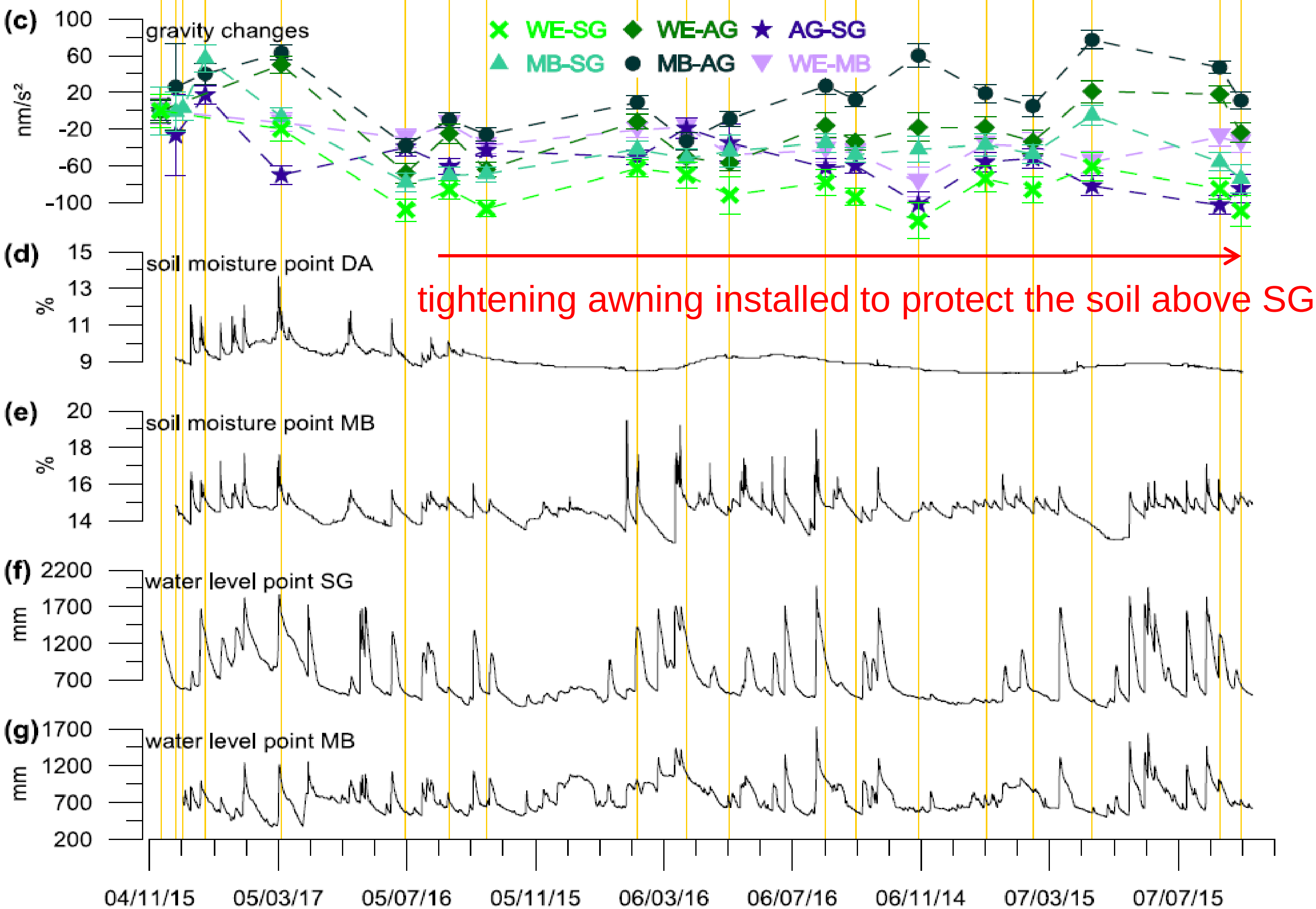

Figure 3.17: Temporal changes in the gravity differences with standard deviation and some hydrological parameters at the observation points: **(a)** gravity changes between different points in the valley and site *DA* on the observatory roof as well as point *ET* on the hill (cf. Figure 3.12), **(b)** gravity changes between different points in the valley and point *DA*, **(c)** gravity changes between all points in the valley, **(d)** soil moisture variation at point *DA* in 1 m depth, **(e)** soil moisture variation at point *MB* in 1 m depth, **(f)** water level variation at point *SG*, **(g)** water level variation at point *MB*.

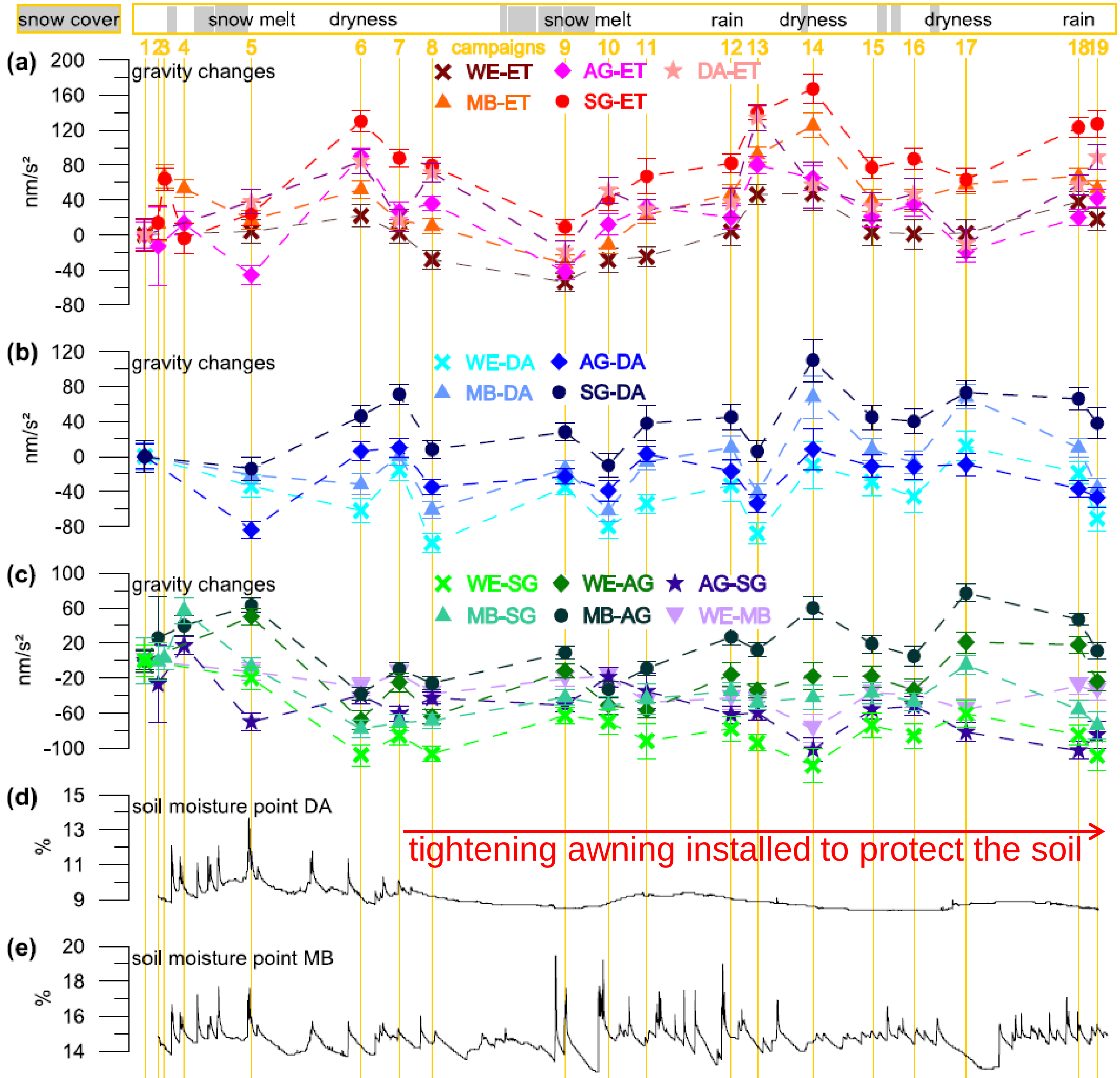

snow cover
snow melt
dryness
snow melt
rain
dryness
dryness
rain
1 2 3 4 5 6 7 8 campaigns 9 10 11 12 13 14 15 16 17 18 19
(a)
gravity changes
WE-ET
AG-ET
DA-ET
MB-ET
SG-ET
nm/s²
(b)
gravity changes
WE-DA
AG-DA
MB-DA
SG-DA
nm/s²
(c)
gravity changes
WE-SG
WE-AG
AG-SG
MB-SG
MB-AG
WE-MB
nm/s²
(d)
soil moisture point DA
%
tightening awning installed to protect the soil
(e)
soil moisture point MB
%

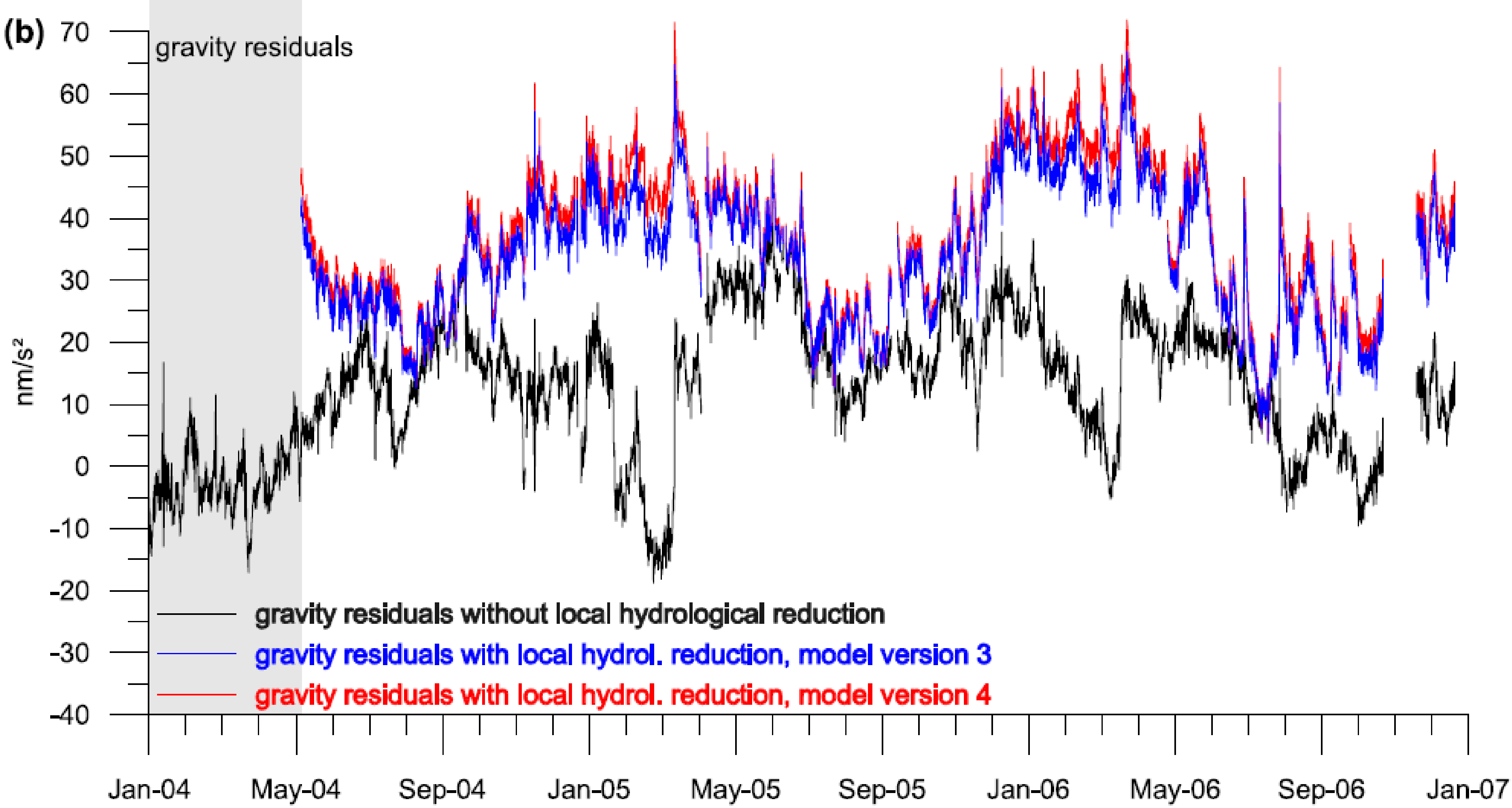

Figure 7.5: Local hydrological effect and gravity residuals: **(a)** local hydrological effect derived from the local hydrological and gravimetric model for the location of the superconducting gravimeter at Moxa observatory; **(b)** gravity residuals of the superconducting gravimeter without and with local hydrological reduction. The grey shaded box marks the initialisation period of the hydrological model.

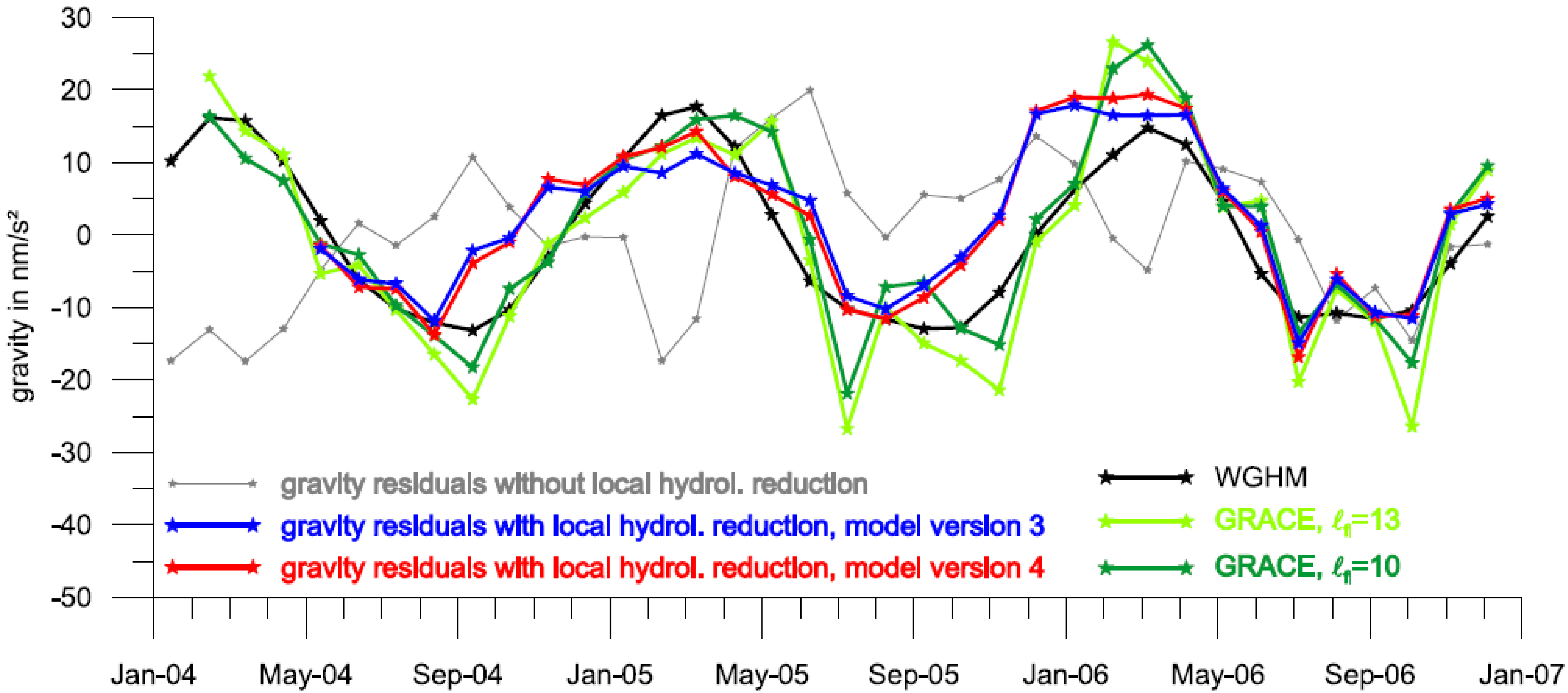

Figure 9.2: Comparison of gravity residuals from the superconducting gravimeter observation, reduced and unreduced for local hydrology, with monthly GRACE solutions using different filtering and gravity variations derived from changes in continental water storage computed with the WGHM model for the station Moxa; GRACE and WGHM data after Neumeyer et al. (2008).

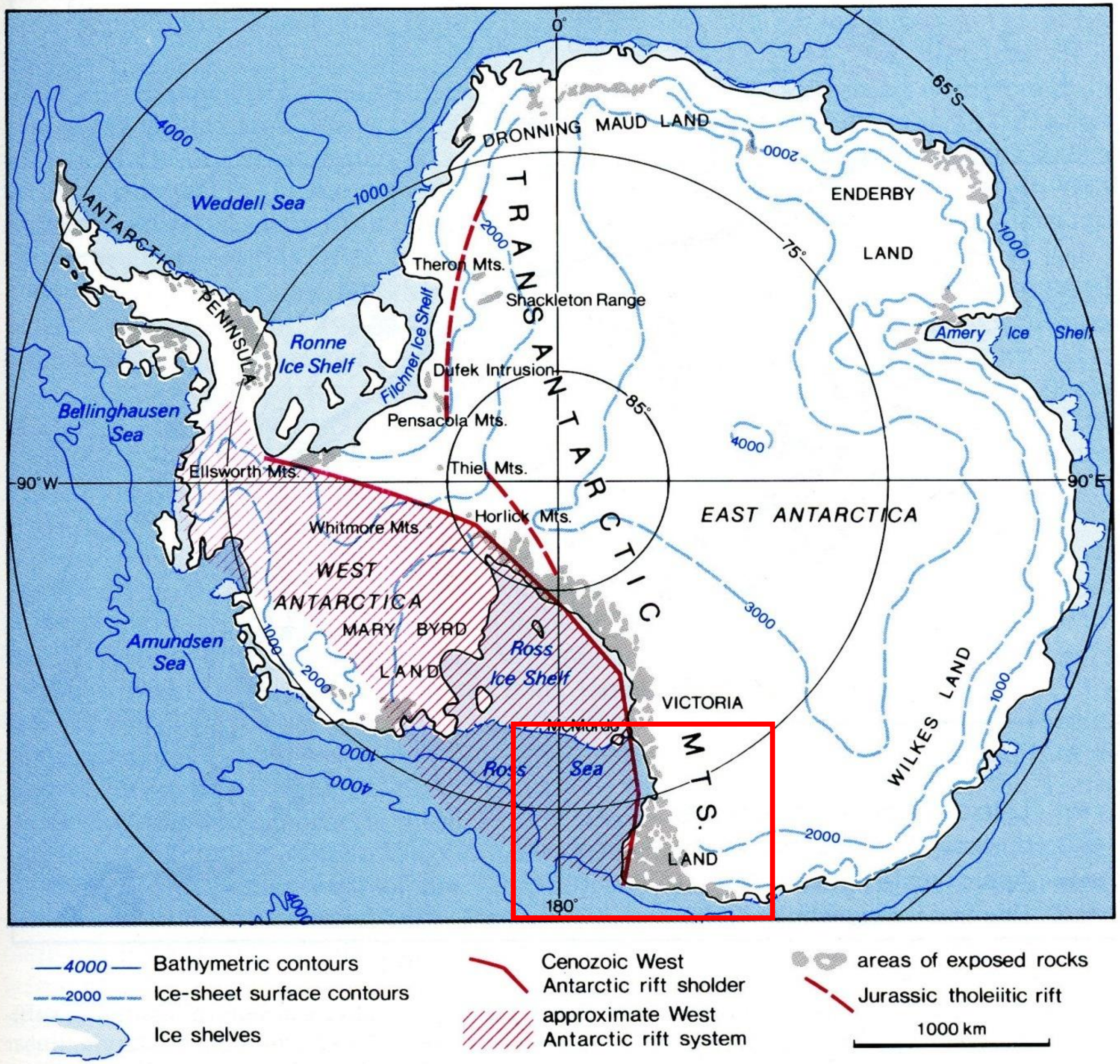

Fig. 1: Index map of Antarctica showing some of the features discussed in the text. The Transantarctic Mountains extend across the continent from Victoria Land near the Ross Sea to the Theron Mountains near the Weddell Sea and comprise the ranges shown by the heavy dashed line as well as those bordering the Ross Embayment. Shaded area is approximate location of West Antarctic rift system. Heavy line is approximate rift shoulder. To conform with convention and other publications, maps of Figs. 1, 2, & 8 (covering all or large regions of Antarctica) have grid north (parallel to the 0° Meridian) at top; all other larger scale maps have normal convention. All maps use polar stereographic projection.

Map of Antartica with Northern Victoria Land marked by the red square

(from Behrendt et al., 1993).

The Italian polar transport ship ITALICA
In Lyttleton, near Christchurch, NZ

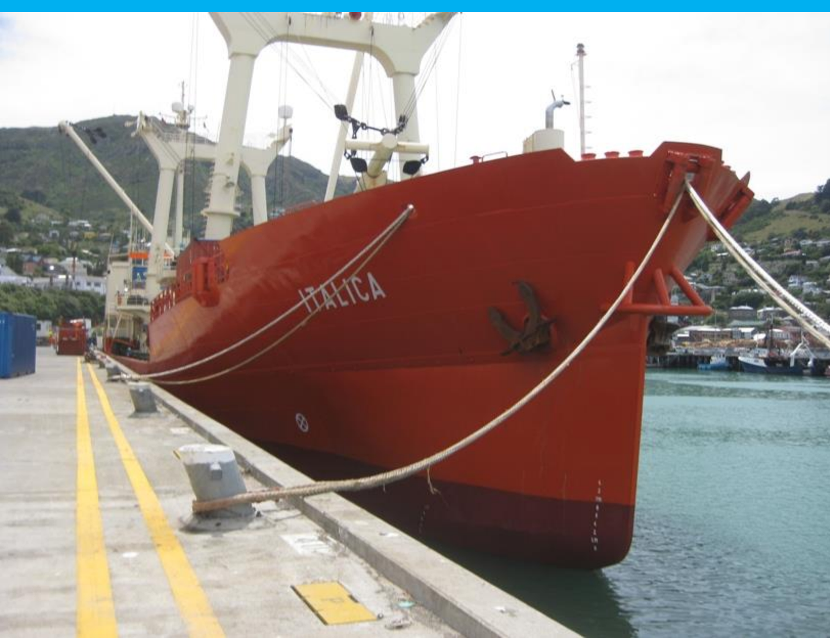

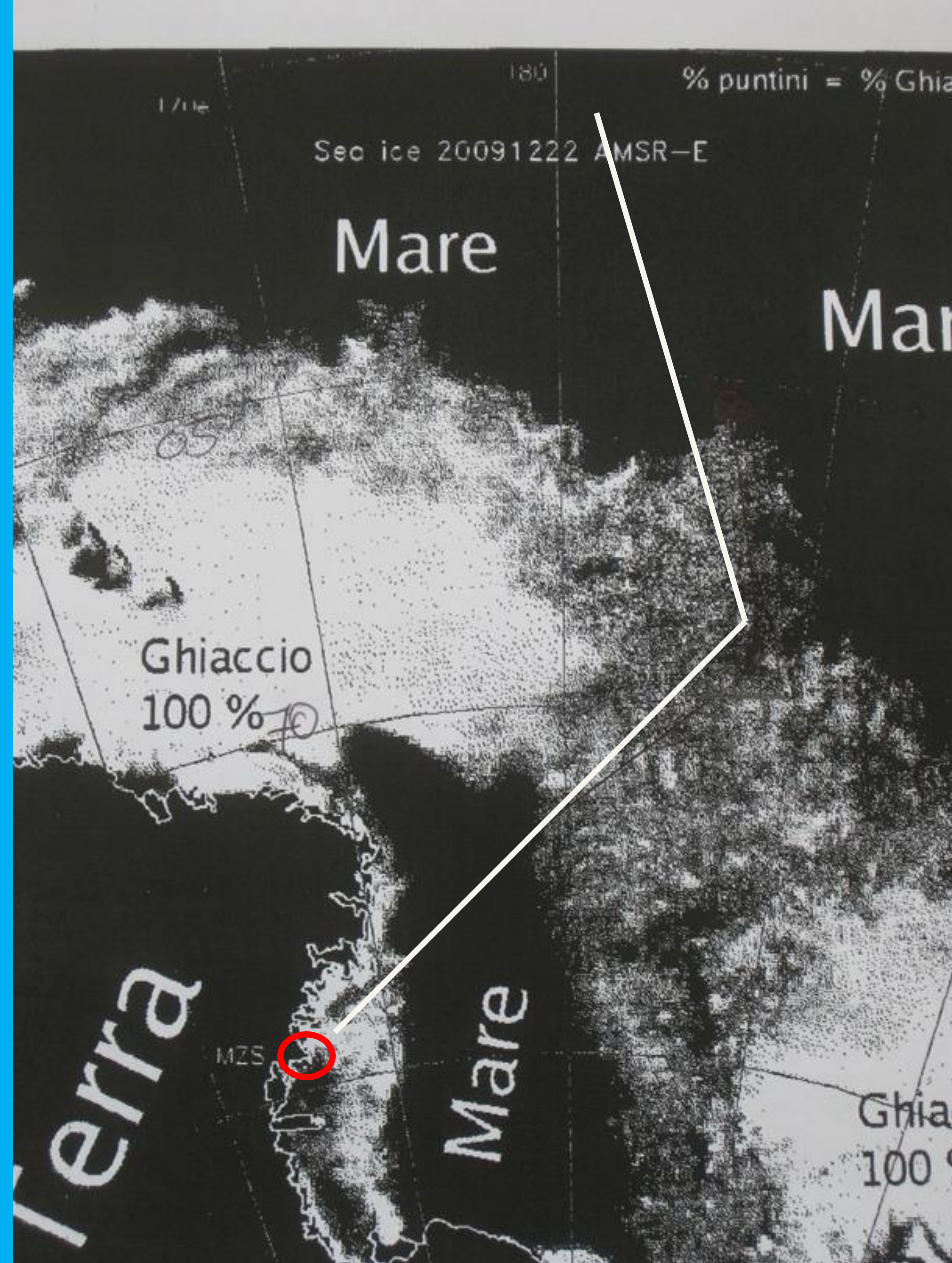

Through the ice to an active volcano, Mt. Melbourne, at Terra Nova Bay:

Comparison of gravity fields off-shore derived from different sources:

Left: Marine measurements and satellites (Bouguer anomaly; BGR)

Right: Satellite altimetry – **note higher resolution** (free air anomaly; KMS)

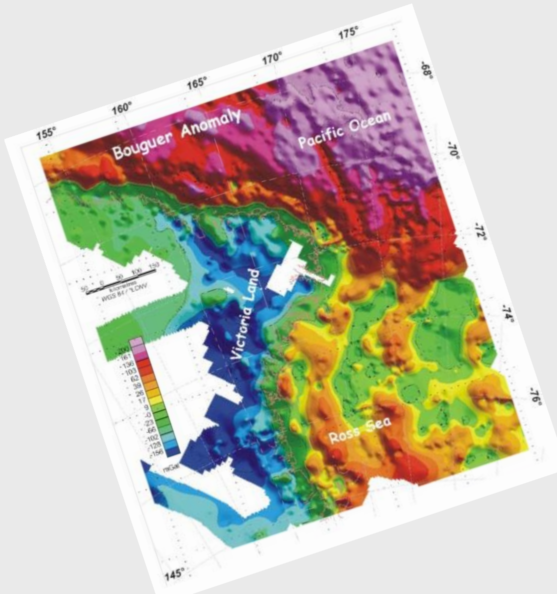

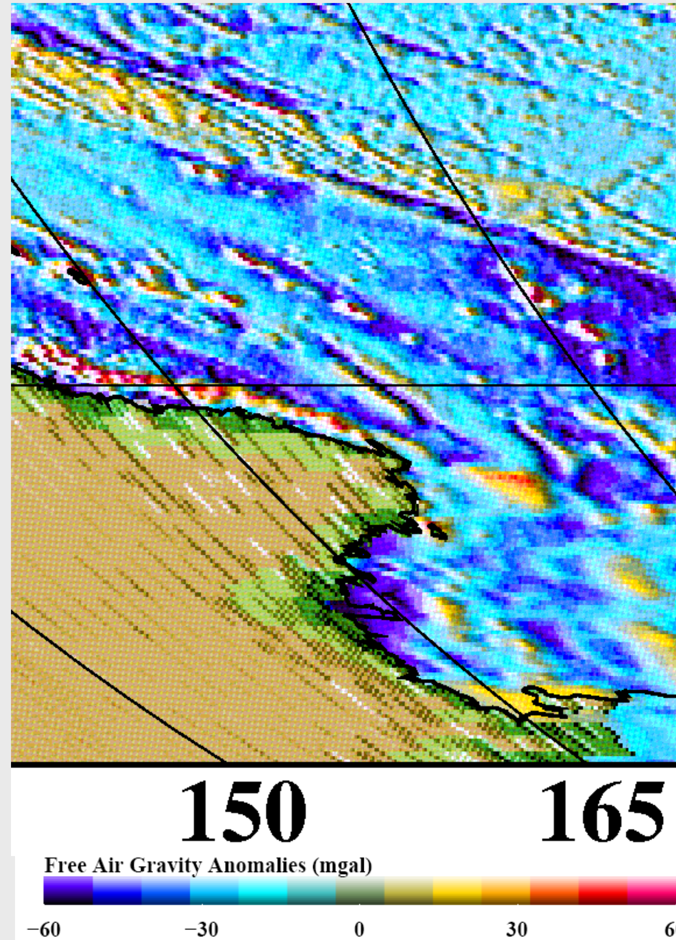

Marine gravity fields (left, Bouguer anomaly based on Sandwell, 1990) and the new gravity field (right, section from the global map free-air anomaly, from Andersen et al., 2005). On-shore Bouguer gravity anomaly map (left) was compiled from different sources (GANOVEX VIII homepage: Gravity survey at the Oates Coast).

VLNDEF:

the network:

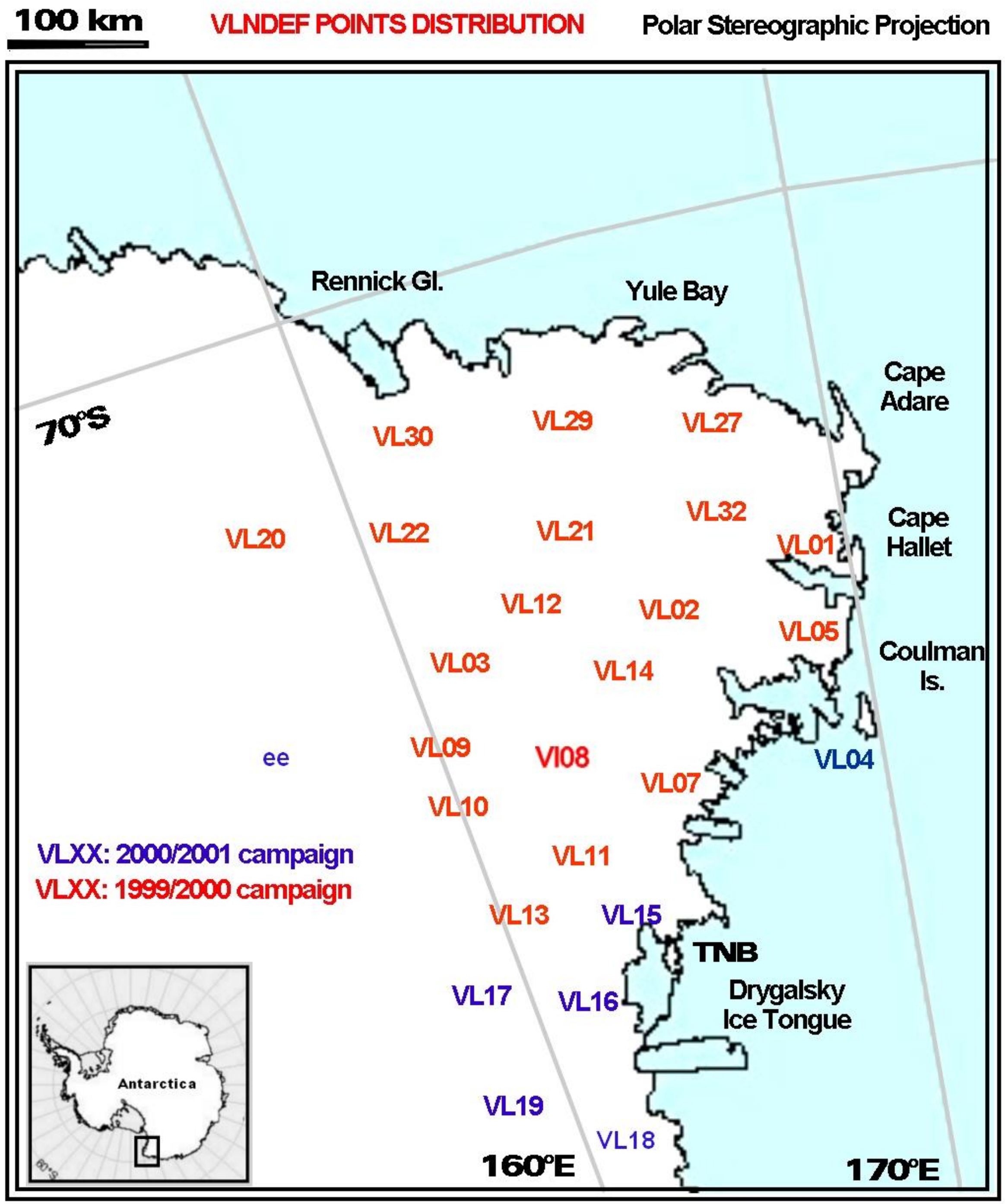

VLNDEF: Documentation

	GPS Geodetic VLNDEF
	Point VL14
	Site Location: Mt Kinet
	USGS Reference Map (1 250.000): Mt. Murchison

Coordinate

WGS84 Cartesian	WGS84 Geodetic
x = -1791154.862	φ = - 73 13 41.68688
y = 449717.697	λ = 165 54 20.50687
z = -6086636.328	h = 2084.050

Benchmark photo

Quotation sketch (quotation in mm)

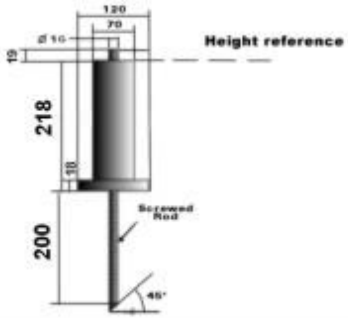

Site description

Point located on an outcrop of the Mt. Kinet ridge toward the Meander Glacier. The benchmark is besides an 8 meters higher outcrop at a distance of 200 meters from the top of the Kinet. The soil is biotitic gneiss rock.

	GPS Geodetic VLNDEF
	Point VL14
	Site Location: Mt Kinet
	USGS Reference Map (1 250.000): Mt. Murchison

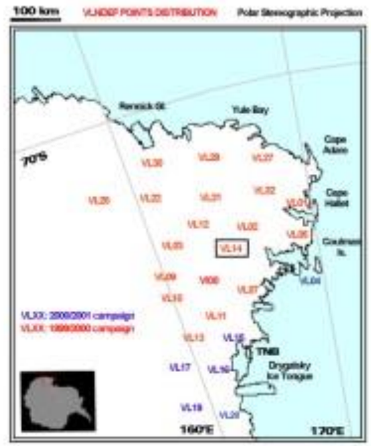

Portion of USGS reference map

Station view

Fig. 4 from Cabra et al. (2007): Absolute horizontal movements derived from observations carries out between December 1999 and January 2003; values in mm/yr and error-circles for a significance level of 95%.

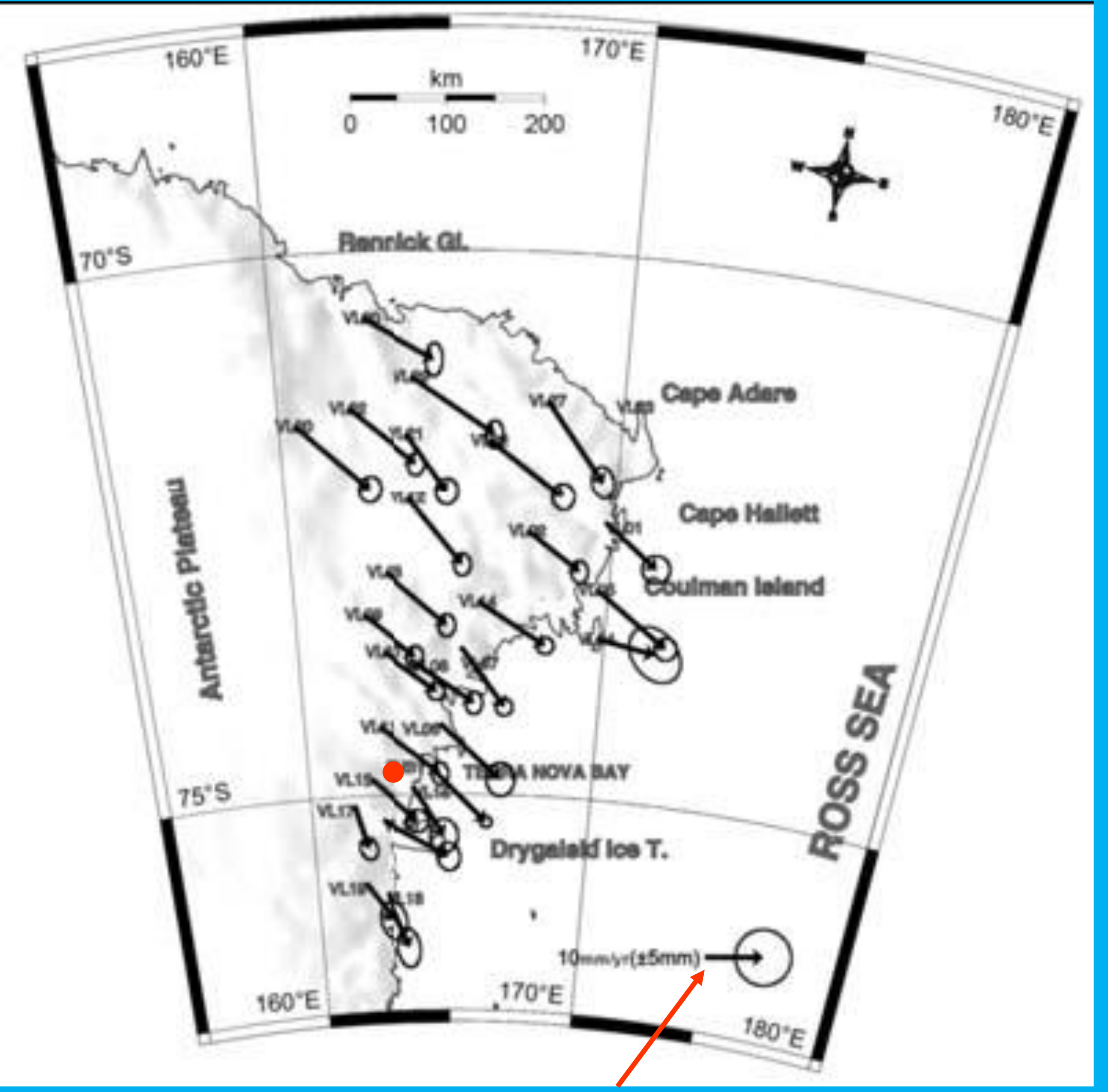

- TNB1

Permanent GPS-station

scale

Fig. 5 aus Cabra et al. (2007): from Cabra et al. (2007): Absolute horizontal movements derived from observations carries out between December 1999 and January 2003; values in mm/yr and error-circles for a significance level of 95%.

Residual velocities after subtraction of the movement of TNB1:

Vnorth = - 10.6 mm/yr,
Veast = +10.6 mm/yr,
Vup = + 0.4 mm/yr.

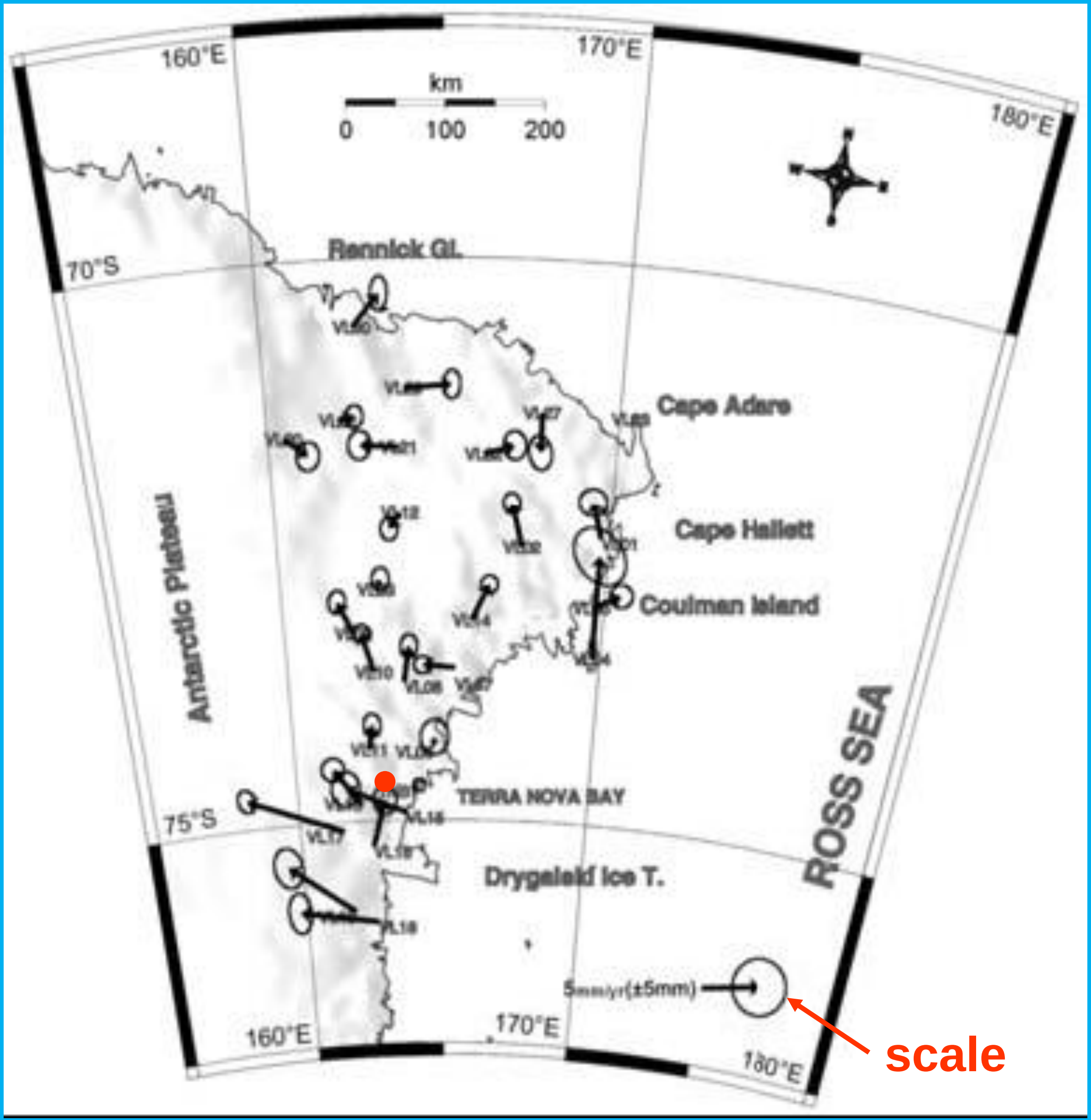

● TNB1 permanent GPS-station

First results for horizontal and vertical deformations obtained from the VLNDEF Network:

published by Cabra et al. (2007):

absolute horizontal velocities are between

17 mm/yr and 8 mm/yr with higher values in the North, and
+1.3 mm/yr as mean vertical crustal movements;

Residual movements after subtraction of the values for TNB1 are:

Vnorth = - 10.6 mm/yr, Veast = +10.6 mm/yr,
Vup = + 0.4 mm/yr (± 0.1).

Aims of the micro-gravity measurements are:

1. Installation of a network of precise gravity differences;
2. Identification of temporal gravity changes – if any;
3. Improvement of the undertanding of neotectonic movements by comparison of the obtained elevation and gravity changes;
4. Monitoring of the changes of the ice cover.

Micro-gravimetry:

station-distribution

Code:
GONDWANA – GDW
20 - VL06
21 - TNB / TNB1
23 - VL08
26 - VL15
28 - VL10
29 - VL18
30 - VL16
31 - VL11
33 - VL13
34 - VL09
36 - VL19
37 - VL17

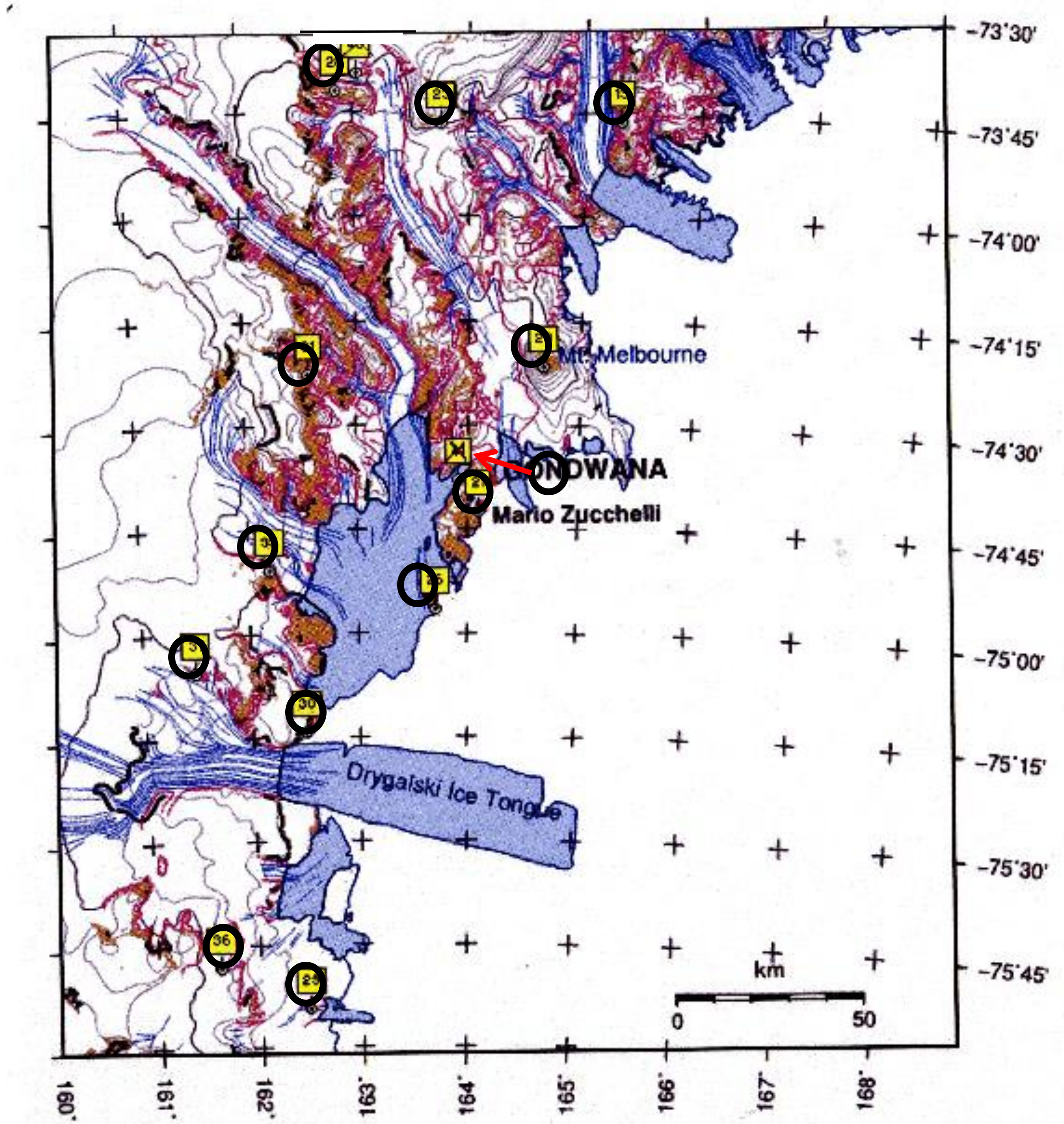

Map created by
M. Scheinert

The start:

Tests of the gravimeters at the station GONDWANA

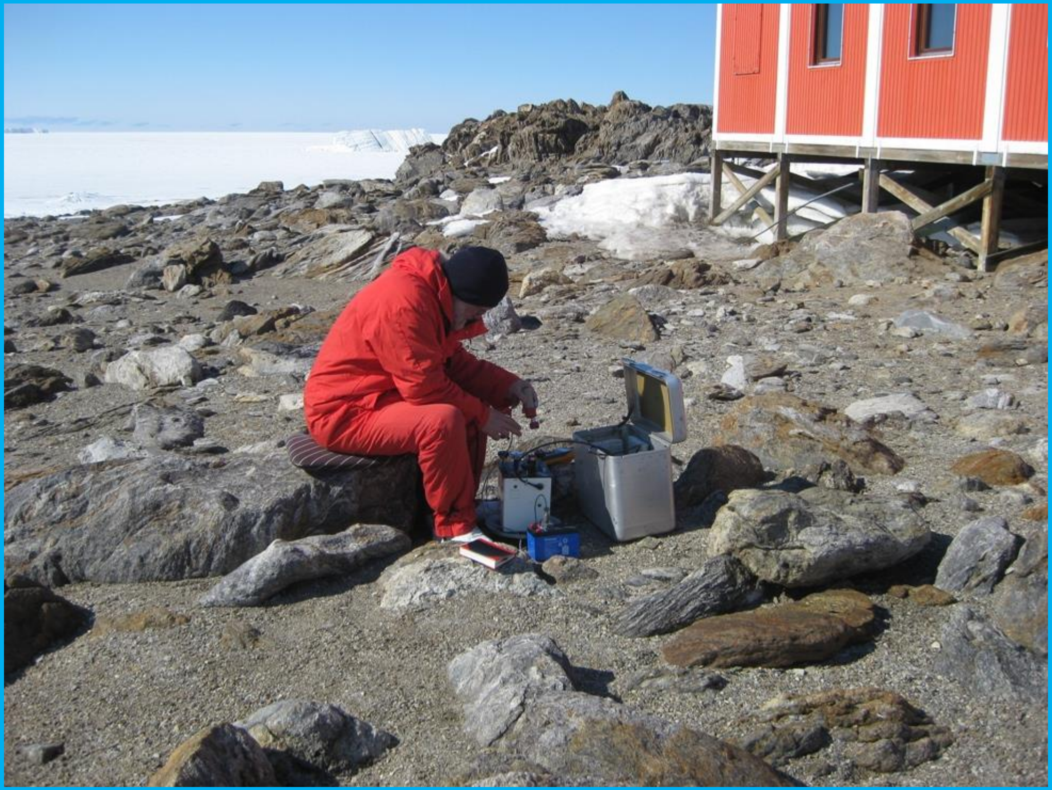

Examples of GPS points Inexpressible Island:

and Cape Philippi:

Mt. Monteagle, 2 655 m, Annäherung von Süden:

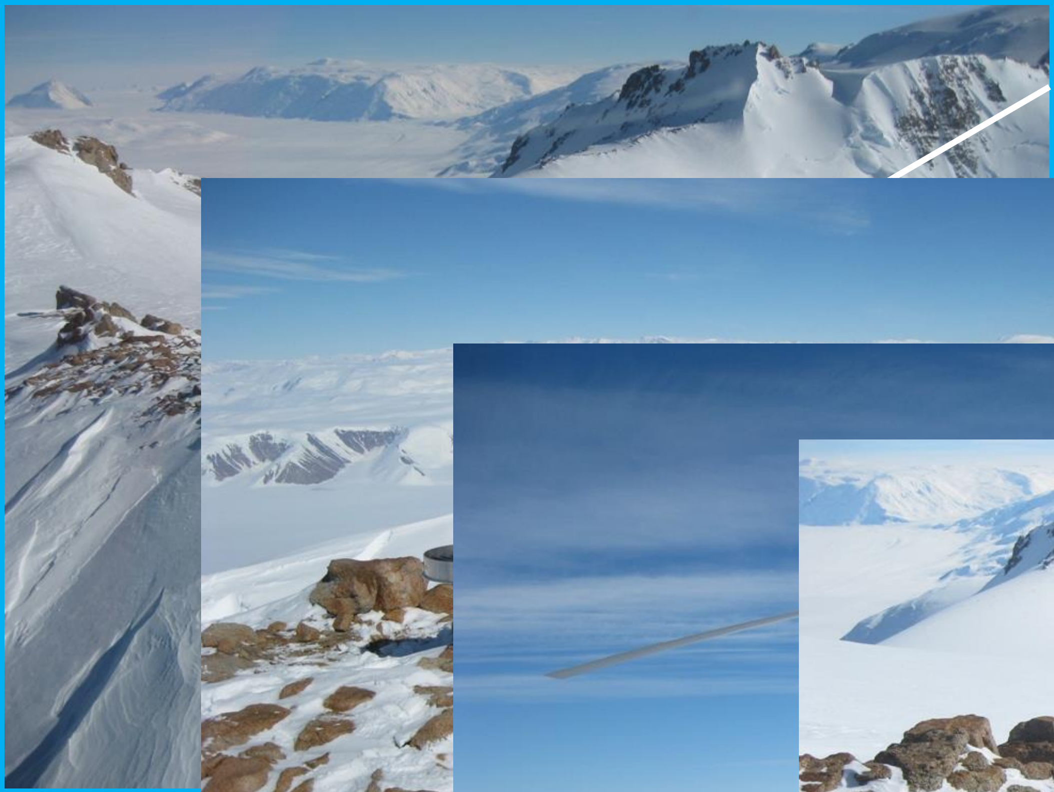

zuerst werden die GPS-Geräte der italienischen Kollegen sichtbar:

GPS-Antenne, Recorder, und Solar Pannel.

Landung nahe am Punkt und Ausladen der Gravimeter.

At Mt. Jiracek, 2 619 m, the conditions are not so good:

The point is on the edge of a cliff:
We had to climb over very rough granite.

Measurements just before termination because of a threatening white-out from behind.

Reference point

The pilot urges us to finish

Catabatic winds from polar plateau

Results

Name	GPS-No.	Connections	Δg (nm/s^2)	rms (nm/s^2)
Gondwana	GOND	80	0	49
Terra Nova building	TNB	24	60,675	98
Terra Nova Ref.	TNB1_GPS	6	−174,128	191
Mt. Melbourne	VL06_GPS	6	−6,898,447	171
Mt. Monteagle	VL07_GPS	17	−5,700,586	110
Mt. Jiracek	VL08_GPS	16	−7,561,680	117
Archambault Ridge	VL10_GPS	12	−7,889,645	136
Mt. Baxter	VL11_GPS	12	−6,702,274	132
Mt. Larsen	VL13_GPS	14	−4,619,520	122
Inexpressible Island	VL15_GPS	16	132,199	109
Cape Philippi	VL16_GPS	16	−1,367,577	112
Evans height	VL17_GPS	15	−2,771,065	115
Starr Nunatak	VL18_GPS	18	−570,838	107
Mc Daniel Nunatak	VL19_GPS	11	−2,426,388	135

Conclusions:

Micro-gravity measurements are best carried out with several gravimeters in parallel in the case of L&R gravimeters;

these measurements allow to work at the threshold of the resolution of the gravimeters because no terrain corrections are needed;

such measurements can be carried out also under unfavourable conditions.

Last point: The Automated Burris gravimeter:

Two examples for daily drift including

Two examples for daily drift including

- long car transport and

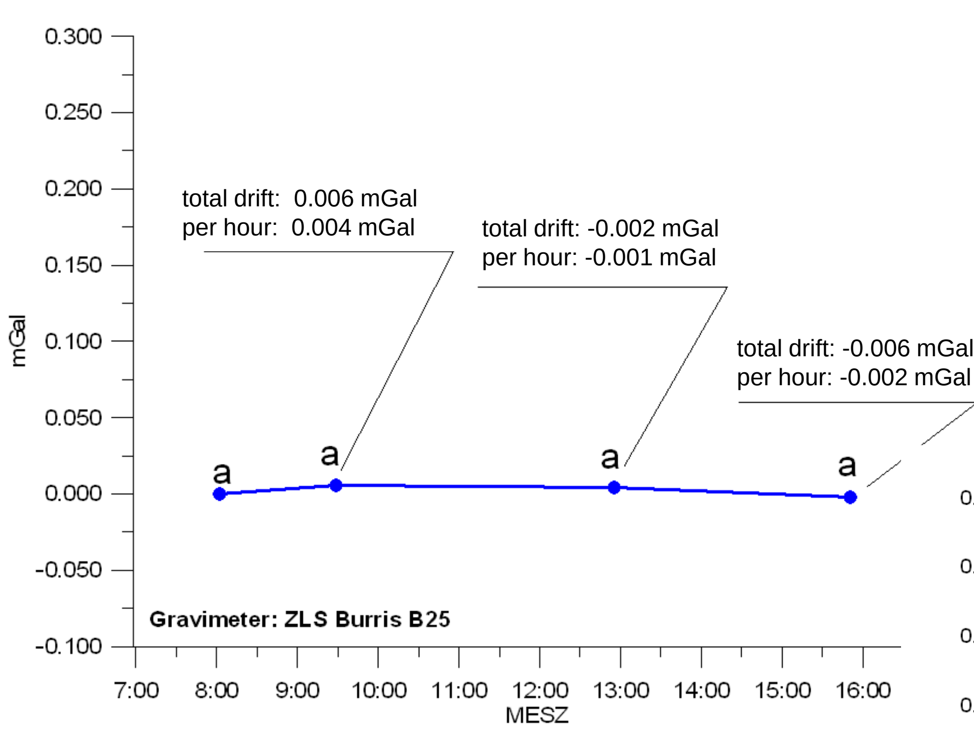

- a strong earthquake:

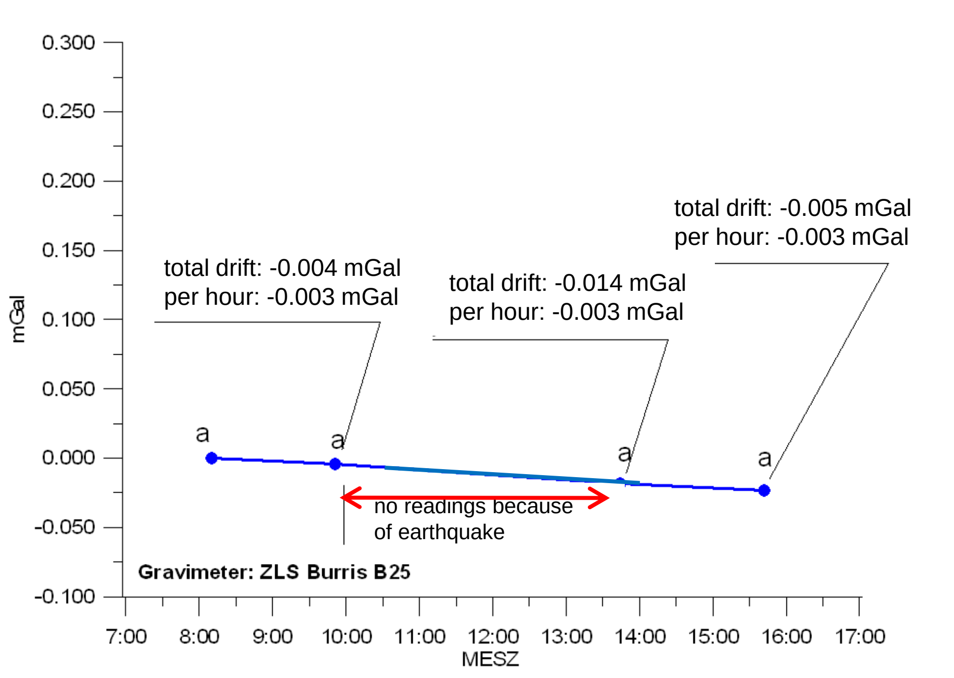

Together with the new control software developed by H.R. Schulz very stable measure-ments are possible, even better than with the PDA of ZLS. **With this software we have a real microgal gravimeter, and the use of several gravimeters in parallel is no longer necessary.**

Thank you !